



**HAL**  
open science

# Geodynamic evolution of the SW Variscides: Orogenic collapse shown by new tectonometamorphic and isotopic data from western Ossa-Morena Zone, SW Iberia

F.M. Rosas, F.O. Marques, Michel Ballevre, C. Tassinari

## ► To cite this version:

F.M. Rosas, F.O. Marques, Michel Ballevre, C. Tassinari. Geodynamic evolution of the SW Variscides: Orogenic collapse shown by new tectonometamorphic and isotopic data from western Ossa-Morena Zone, SW Iberia. *Tectonics*, 2008, 27 (6), pp.TC6008. 10.1029/2008TC002333 . insu-00352997

**HAL Id: insu-00352997**

**<https://insu.hal.science/insu-00352997>**

Submitted on 29 Jun 2016

**HAL** is a multi-disciplinary open access archive for the deposit and dissemination of scientific research documents, whether they are published or not. The documents may come from teaching and research institutions in France or abroad, or from public or private research centers.

L'archive ouverte pluridisciplinaire **HAL**, est destinée au dépôt et à la diffusion de documents scientifiques de niveau recherche, publiés ou non, émanant des établissements d'enseignement et de recherche français ou étrangers, des laboratoires publics ou privés.

# Geodynamic evolution of the SW Variscides: Orogenic collapse shown by new tectonometamorphic and isotopic data from western Ossa-Morena Zone, SW Iberia

F. M. Rosas,<sup>1</sup> F. O. Marques,<sup>2</sup> M. Ballèvre,<sup>3</sup> and C. Tassinari<sup>4</sup>

Received 19 May 2008; revised 16 July 2008; accepted 28 August 2008; published 11 December 2008.

[1] The pre-Mesozoic geodynamic evolution of SW Iberia has been investigated on the basis of detailed structural analysis, isotope dating, and petrologic study of high-pressure (HP) rocks, revealing the superposition of several tectonometamorphic events: (1) An HP event older than circa 358 Ma is recorded in basic rocks preserved inside marbles, which suggests subduction of a continental margin. The deformation associated with this stage is recorded by a refractory graphite fabric and noncoaxial mesoscopic structures found within the host metasediments. The sense of shear is top to south, revealing thrusting synthetic with subduction (underthrusting) to the north. (2) Recrystallization before circa 358 Ma is due to a regional-scale thermal episode and magmatism. (3) Noncoaxial deformation with top to north sense of shear in northward dipping large-scale shear zones is associated with pervasive hydration and metamorphic retrogression under mostly greenschist facies. This indicates exhumation by normal faulting in a detachment zone confined to the top to north and north dipping shear zones during postorogenic collapse soon after 358 Ma ago (inversion of earlier top to south thrusts). (4) Static recrystallization at circa 318 Ma is due to regional-scale granitic intrusions. **Citation:** Rosas, F. M., F. O. Marques, M. Ballèvre, and C. Tassinari (2008), Geodynamic evolution of the SW Variscides: Orogenic collapse shown by new tectonometamorphic and isotopic data from western Ossa-Morena Zone, SW Iberia, *Tectonics*, 27, TC6008, doi:10.1029/2008TC002333.

## 1. Introduction

[2] The Variscan orogen in western Europe (Figure 1a) has been interpreted as the result of late Paleozoic collision

between a part of NW Gondwana, and a continent to the NW, possibly Baltica or North America [Brun and Burg, 1982; Burg *et al.*, 1987; Ribeiro *et al.*, 1990; Quesada, 1991; Quesada *et al.*, 1991, 1994]. Continental collision followed earlier subduction and subsequent closure of an intervening ocean (Rheic), culminating in the formation of a major arcuate orogenic belt: the Ibero-Armorican Arc (IAA, Figure 1a) [Matte and Ribeiro, 1975; Matte, 1986; Dias and Ribeiro, 1995; Ribeiro *et al.*, 1995]. This large-scale structure is characterized by complex crustal imbrication and tectonic piling due to orthogonal convergence in the frontal areas of the IAA (now preserved in NW Iberia) and by dextral and sinistral transpression in Armorica and SW Iberia, respectively.

[3] The pre-Mesozoic geodynamic evolution of SW Iberia is still not well understood because a great deal of information is still missing regarding structure/tectonics, petrology (igneous and metamorphic), geochemistry, isotopic dating and palinspastic reconstruction. However, the recognition of major terranes in SW Iberia seems consensual and comprises (Figure 1b), from SW to NE, the South Portuguese Terrane (SPT), an ophiolitic terrane (which includes the Pulo do Lobo Unit and the Beja-Acebuches Ophiolitic Complex, BAOC) and the Iberian Terrane, which in SW Iberia corresponds mostly to the Ossa-Morena Zone (OMZ). The boundary between the OMZ and the SPT has been interpreted as a major Variscan suture in SW Iberia, because it comprises ophiolitic rocks of the BAOC and Pulo do Lobo Unit, accreted to the Iberian Terrane during northward subduction of the Rheic [Munhá *et al.*, 1986; Matte, 1986, 1991; Crespo-Blanc and Orozco, 1988; Ribeiro *et al.*, 1990; Quesada, 1990, 1991, 1992; Crespo-Blanc, 1992; Fonseca and Ribeiro, 1993; Quesada *et al.*, 1991, 1994; Fonseca *et al.*, 1999]. The best preserved structures affecting both BAOC ophiolitic rocks and the northern adjacent OMZ continental domains exhibit top to north sense of shear, which has been interpreted as thrusting before the present work [e.g., Fonseca and Ribeiro, 1993; Quesada *et al.*, 1994; Fonseca *et al.*, 1999; Ribeiro *et al.*, 2007]. Peak metamorphic conditions in the OMZ comprise high-pressure/medium-temperature (HP/MT) in the west [Fonseca *et al.*, 1999] and HT/LP in the Aracena Metamorphic Belt (AMB, Figure 1b), to the east [e.g., Bard, 1977; Díaz Azpiroz *et al.*, 2006, and references therein]. Such differences and lack of more complete information show the great need for further study and clarification concerning the regional tectonometamorphic evolution of the SW Iberian Variscan orogen.

<sup>1</sup>Departamento de Geologia and LATTEX-IDL, Faculdade Ciências, Universidade Lisboa, Lisbon, Portugal.

<sup>2</sup>Departamento de Geologia and CGUL-IDL, Faculdade Ciências, Universidade Lisboa, Lisbon, Portugal.

<sup>3</sup>Géosciences-Rennes, UMR6118, Université de Rennes, Campus de Beaulieu, CNRS, Rennes, France.

<sup>4</sup>Centro de Pesquisas Geocronológicas da Universidade de São Paulo, São Paulo, Brazil.

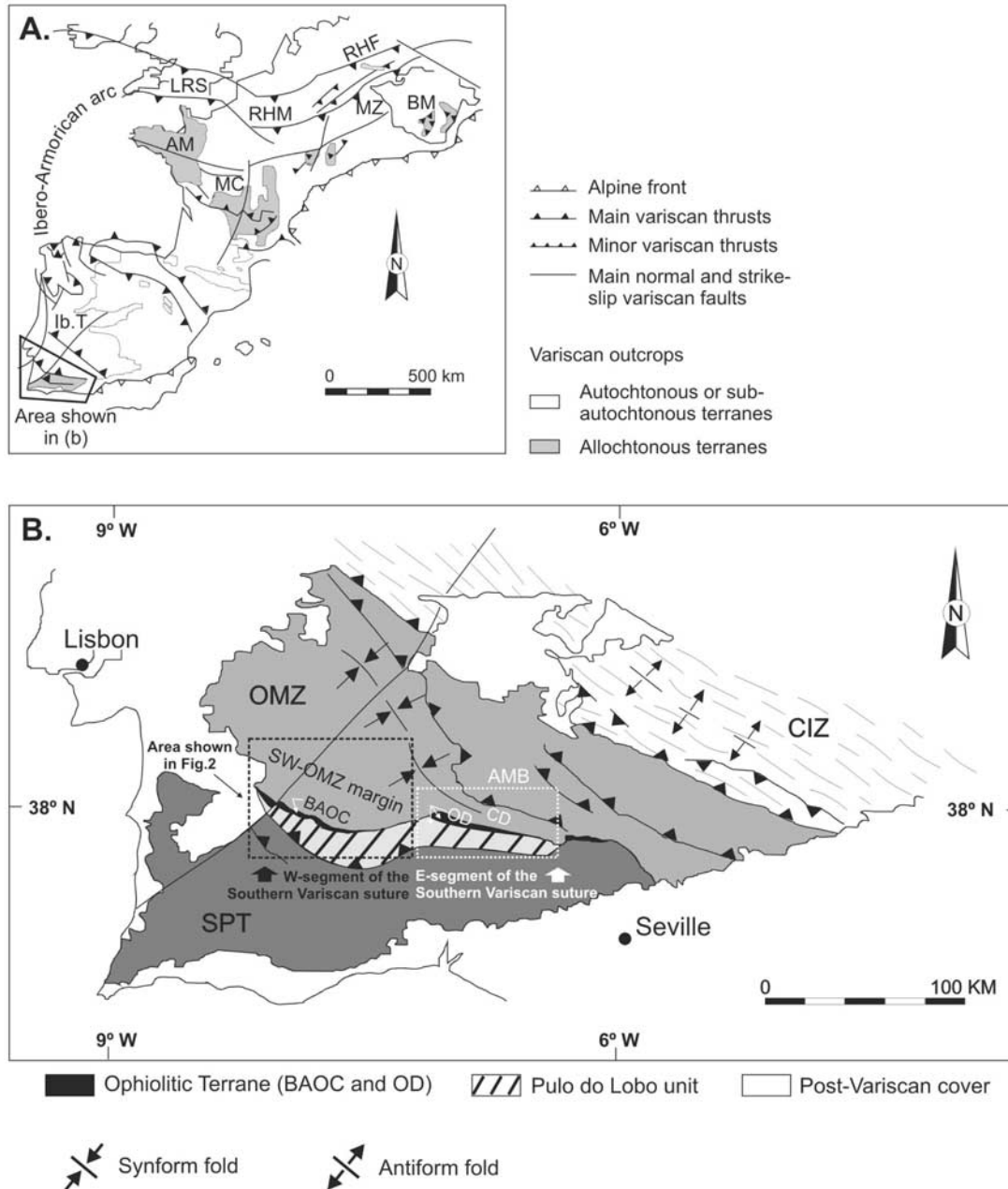


**Figure 1.** (a) Main units in the European Variscan belt (modified after *Díaz Azpiroz et al.* [2006]). Ib.T, Iberian terrane; AM, Armorican massif; MC, Massif central; RHM, Rheno-Hercynian massif; MZ, Moldanubian zone; BM, Bohemian massif; LRS, Lizard-Rheic suture; RHF, Rheno-Hercynian front. (b) Main terranes in SW Iberian Variscan belt with location of the area depicted in Figure 2 (modified after *Julivert et al.* [1974] and *Díaz Azpiroz et al.* [2006]). CIZ, Central Iberian zone; OMZ, Ossa-Morena zone; SPT, South Portuguese terrane; BAOC, Beja-Acebuches ophiolitic complex; AMB, Aracena metamorphic belt; OD, oceanic domain; CD, continental domain.

**Figure 2.** (a) Structural-geological map of the western segment of the southern Variscan suture (see location in Figure 1b) (background geological map modified after *Oliveira et al.* [1992] and structural data from the present study). (b) Schematic cross section of the southern branch of the Iberian Massif (SW OMZ), depicting the crustal architecture of the OMZ-SPZ suture zone. SPT, South Portuguese Terrane; PLT, Pulo do Lobo Terrane; OMZ, Ossa-Morena Zone; BAOC, Beja-Acebuches Ophiolitic Complex; BIC, Beja Igneous Complex. Structural data are from *Fonseca and Ribeiro* [1993], *Araújo et al.* [2005], and present work.

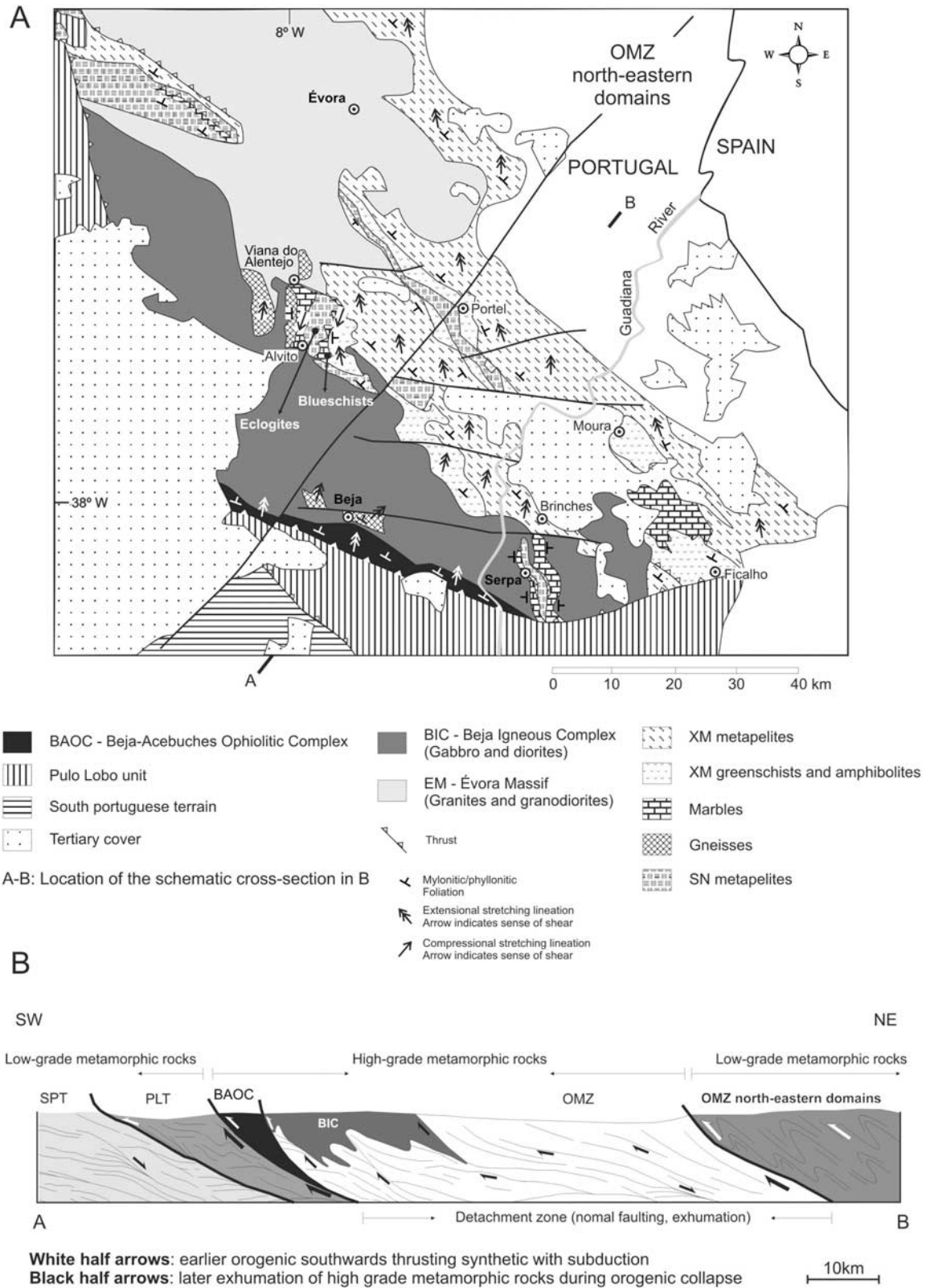


Figure 2

**Table 1.** Summary of Isotopic Data for SW OMZ

Authors	Location (Unit)	Method	Rock	Age, Ma
<i>Dallmeyer et al.</i> [1993]	BIC gabbro-diorites	$^{40}\text{Ar}/^{39}\text{Ar}$ hornblende	gabbro	342–346
<i>Castro et al.</i> [1999]	Beja and Aracena	$^{40}\text{Ar}/^{39}\text{Ar}$ hornblende	gabbro and amphibolite	circa 343 and circa 328
<i>Pin et al.</i> [1999]	BIC gabbro-diorites	U/Pb zircon	gabbro	350 ± 4 (S)
<i>Pin et al.</i> [1999]	BIC gabbro-diorites	U/Pb zircon	gabbro	352 ± 4 (T)
Present work	EM granodiorites (38°20'27"N, 7°58'34"W)	K/Ar amphibole	granodiorite	318 ± 11
Present work	AP micaschists (38°15'59"N, 7°56'53"W)	K/Ar muscovite	micaschist	358 ± 11

[4] Previous work in SW OMZ [*Carvalhosa*, 1965, 1972; *Carvalhosa and Zbyszewski*, 1991] led to the general outline of several main cartographic units (Figure 2a): (1) a gneissic unit; (2) a marble unit showing frequent intercalations of different types of metabasic rocks; (3) a metapelitic unit mainly composed of graphitic schists, garnet/quartz-feldspar micaschists and intercalations of different types of metabasic rocks (regionally known as the Série Negra formation, SN); and (4) another metapelitic unit mainly comprising greenschists and micaschists (regionally known as the Xisto de Moura formation, XM). These units are in contact with two main igneous complexes (Figure 2a): a granitic massif (regionally known as the Évora Massif, EM), and a gabbro-dioritic igneous complex to the SW (regionally known as the Beja Igneous Complex, BIC). In SW OMZ, the nature of the contacts between the mapped metasedimentary units is tectonic.

[5] The age of the mapped units is mostly unknown because of the lack of lithostratigraphic markers and isotopic dating. Nevertheless, some authors have suggested a Proterozoic age for the SN micaschists, a Cambrian age for the marbles [*Carvalhosa*, 1972, 1983; *Teixeira*, 1981] and a Silurian age for the XM metapelites [*Piçarra and Gutierrez-Marco*, 1992], mostly based on regional correlations with lithologically similar units in eastern OMZ. Previously, reported isotopic ages focused only on the BIC. *Dallmeyer et al.* [1993] reported  $\text{Ar}^{40}/\text{Ar}^{39}$  cooling ages between circa 342 and 346 Ma, obtained from hornblende concentrates, and *Pin et al.* [1999] reported U/Pb crystallization ages of  $350 \pm 4$  and  $352 \pm 4$  Ma, obtained from zircon concentrates (Table 1).

[6] The main planar-linear tectonic fabric that regionally affects pre-Mesozoic rocks in the SW OMZ has been described as a gently NNE to NE dipping mylonitic foliation with a NNE-SSW trending mineral stretching lineation [*Fonseca and Ribeiro*, 1993; *Araújo et al.*, 2005]. This tectonic fabric was attributed to a first deformation phase (D1 of *Fonseca and Ribeiro* [1993] and *Araújo et al.* [2005]), although it is not at the highest metamorphic grade. The deduced sense of shear is top to north. Locally N-S trending folds occur close to the contact with the stronger BIC and show an anomalous orientation relative to the general trend of the SW Variscan suture (e.g., Serpa and Alvito structures, Figure 2a).

[7] Previous work on metamorphic evolution and geochemistry focused mainly on HP metabasites [*Fonseca et al.*, 1993, 1999], on BIC and on some marbles [*Gomes*, 2000]. However, the mineral assemblages defining the pervasive foliation and associated microstructures observed

in the country rock units generally show retrogression under greenschist facies conditions. BIC rocks show a calc-alkaline signature [e.g., *Ribeiro et al.*, 1979; *Martinez and Ibarguchi*, 1983; *Santos et al.*, 1987, 1990; *Quesada et al.*, 1994; *Jesus et al.*, 2007, and references therein], which has been interpreted as evidence for orogenic magmatism associated with northward subduction beneath the SW OMZ margin. *Fonseca et al.* [1993, 1999] have suggested that the eclogites evolved from  $\sim 450\text{--}500^\circ\text{C}/1.0\text{--}1.2$  GPa to  $\sim 650^\circ\text{C}/1.4\text{--}1.6$  GPa (eclogite facies), before being retrogressed to  $\sim 600\text{--}500^\circ\text{C}/1.1\text{--}0.6$  GPa (barroisitic stage) and  $\sim 400\text{--}500^\circ\text{C}/0.4\text{--}0.5$  GPa (greenschist/epidote-amphibolite facies). *Fonseca et al.* [1999] proposed that the mafic eclogite protholiths derive from tholeiitic basaltic magmas of continental affinity, and interpreted this as the result of a contribution of continental crust to ascending MORB-type magmas. Most of the observed rocks record late low-amphibolite to greenschist facies metamorphism, and/or pervasive thermal recrystallization due to two episodes of contact metamorphism [e.g., *Santos et al.*, 1987, 1990; *Dallmeyer et al.*, 1993; *Fonseca et al.*, 1993, 1999; *Pin et al.*, 1999; *Gomes*, 2000; *Rosas*, 2003]. Therefore, their main mineralogical composition and texture reflect these metamorphic conditions, corresponding mostly to granoblastic textures, and only poorly preserved dynamic recrystallized fabrics.

[8] The origin of the rock units in the OMZ is mostly unknown due to the absence of reliable sedimentary, stratigraphic and geochemical constraints. Nevertheless, previous authors agree that the most probable geological setting for the origin of the metasedimentary rocks in the southernmost OMZ domains corresponds to a passive margin, in which the marbles would represent a lower Paleozoic carbonate shelf [e.g., *Quesada*, 1990, 1991, 1992; *Fonseca and Ribeiro*, 1993; *Fonseca et al.*, 1993; *Quesada et al.*, 1994].

[9] In this work, we present new detailed structural/tectonic, petrologic, and isotopic data to constrain the tectonometamorphic evolution of the SW OMZ. Field data show that the gabbro-diorite (BIC) and granodiorite (EM) intrusions have different ages: (1) contact metamorphism due to BIC intrusion affected rocks and structures older than circa 350 Ma, but recrystallized rocks were subsequently affected by post-BIC shear deformation and retrogression and (2) in contrast, the EM granodioritic rocks postdate most pre-Mesozoic deformation in SW OMZ. Therefore, we dated BIC and EM intrusions, and the host rock to constrain the age of the main tectonic events. On the basis of key overprint relationships between structures, on new isotopic data and on the discovery of new evidences of HP meta-

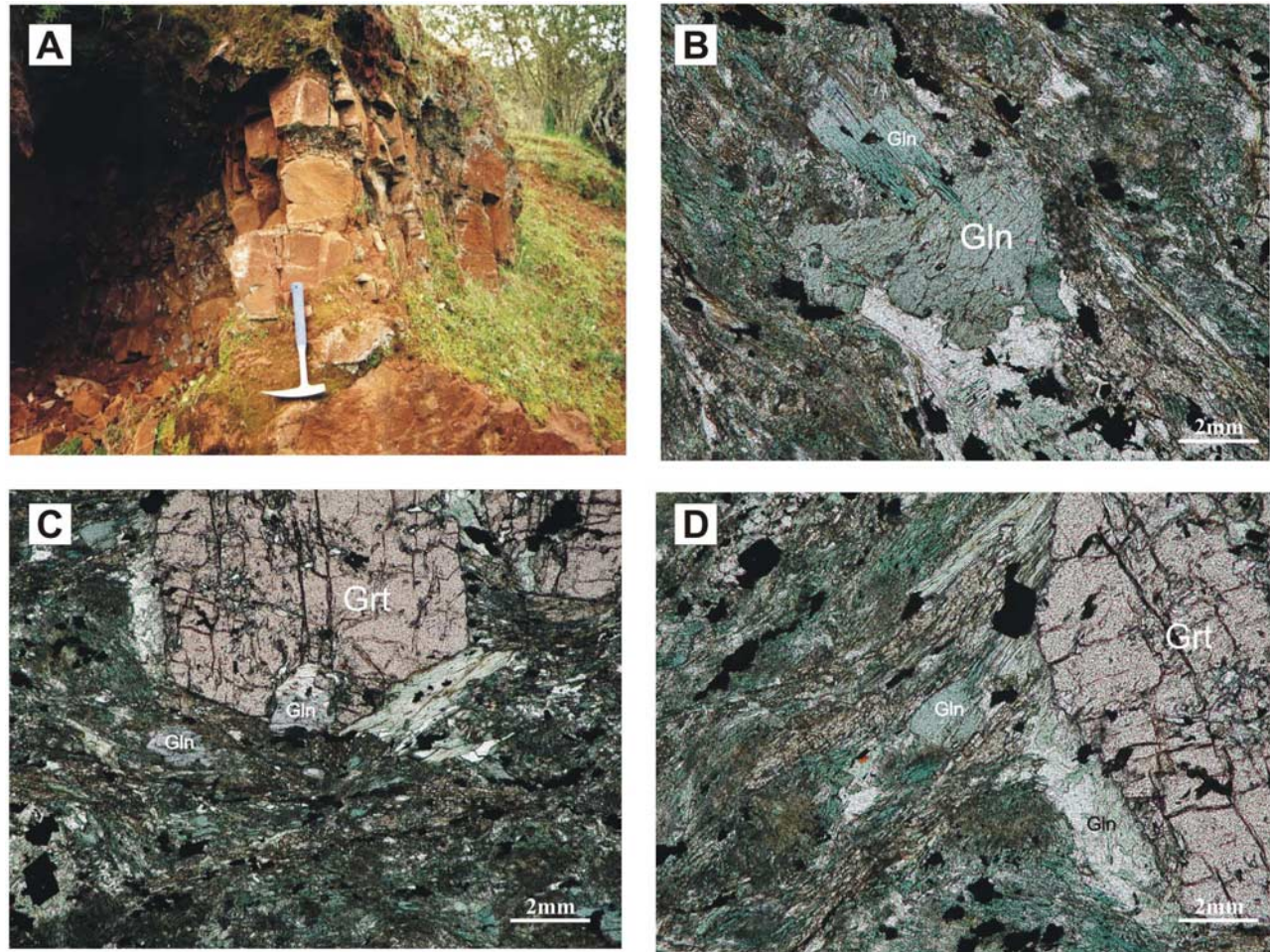


**Figure 3.** Blueschists from the SW OMZ. (a) Outcrop near Alvito (see location in Figure 2). (b to d) Photomicrographs depicting the early HP mineral assemblage, mainly including garnet (Grt) and glaucophane (Gln) preserved inside a retrogressed matrix (greenschist facies) mostly composed of chlorite  $\pm$  actinolite  $\pm$  epidote (cross polarized light, CPL).

morphism, we discuss the previously proposed interpretations for the geodynamic evolution of the SW Iberian Variscan orogen. We show that an alternative interpretation comprising postorogenic collapse and exhumation of high-pressure rocks is more suitable to explain the presently available data.

## 2. Metamorphism

[10] Two types of metamorphism have affected the rocks in SW OMZ: regional and contact metamorphism.

### 2.1. Regional Metamorphism

[11] Despite both metabasic boudins and host rocks (marbles and micaschists) recording the same late retro-metamorphic evolution to low-amphibolite/greenschists facies, some of the metabasites still record an earlier HP metamorphism. This is the case of new findings of blueschists intercalated in sheared marbles (Figures 2 and 3). The blueschists (Figure 3) are characterized by two mineral

assemblages: an early assemblage consisting of garnet (spessartine, pyrope) + blue amphibole (glaucophane) + epidote (pistacite) + quartz + rutile, in which garnet occurs as poikiloblastic idioblastic grains, with small-sized inclusions mainly consisting of quartz, epidote, amphibole and rutile. A later retrogressive assemblage consists of replacement of glaucophane with submicroscopic symplectites and of retrogressive blue-green amphiboles (winchite) overgrowing glaucophane. Matrix rutile is rimmed by ilmenite. Further retrogression is also marked by the growth of abundant pale green chlorite, minor plagioclase and carbonate, and numerous, tiny, square- to lozenge-shaped opaques in the matrix. The early paragenesis (Grt-Gln-Ep-Qtz) is a typical assemblage of blueschist facies [e.g., Evans, 1990], stable in the range 400–500°C, 0.8–1.6 GPa. Unfortunately, it is not possible to give more precise estimates, since classical geothermobarometers are lacking for the studied assemblage. Decompression is marked by the growth of sodic-calcic amphiboles, albite and magnetite, requiring extensive hydration after peak P-T conditions. Because of

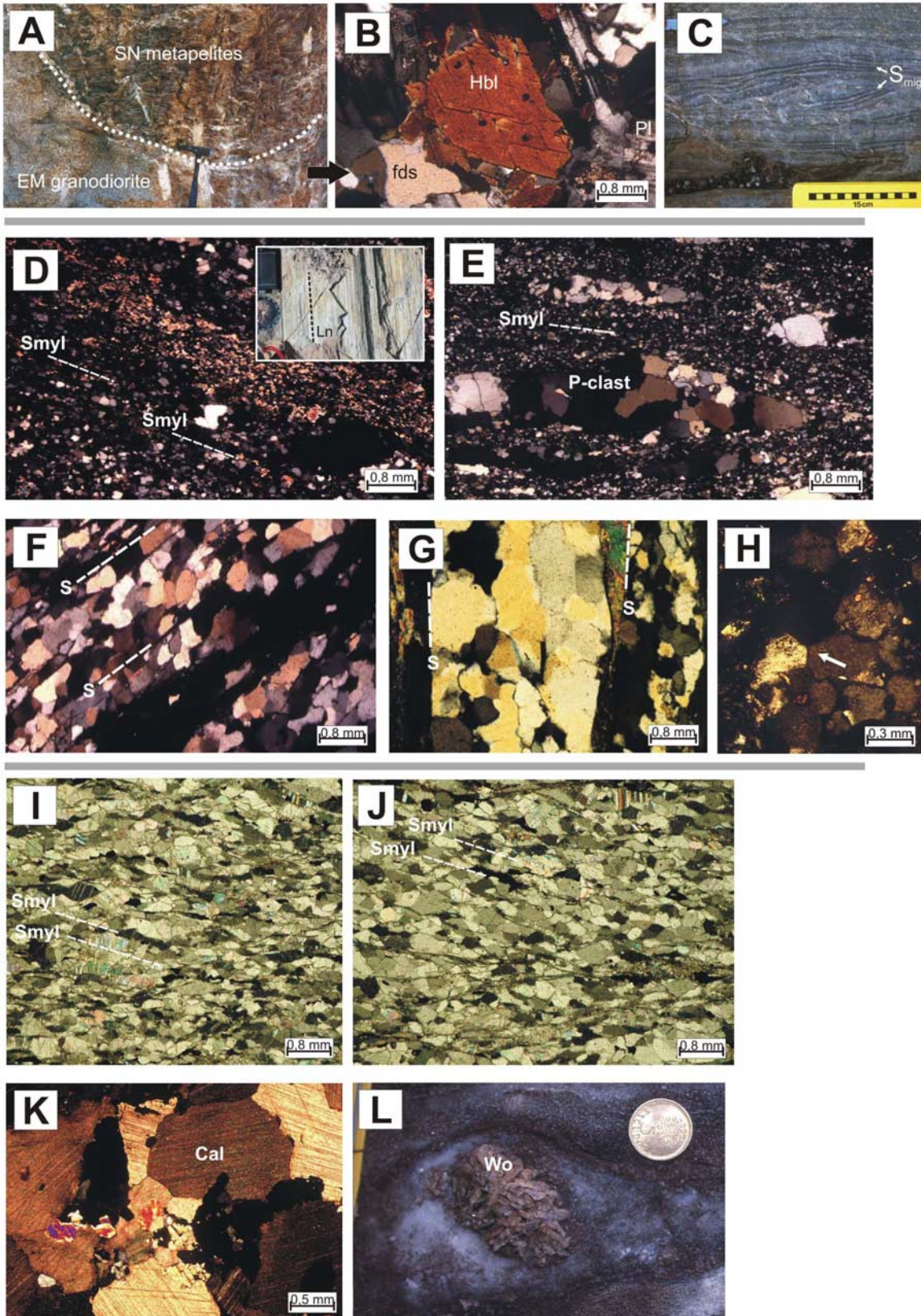


Figure 4

the lack of actinolite, the retrograde paragenesis belongs to the albite-epidote amphibolite facies, rather than to greenschist facies, indicating that retrogression took place at relatively high P-T conditions (about 0.6–0.8 GPa,  $450 \pm 50^\circ\text{C}$ ) [Ernst, 1979]. Chlorite and submicroscopic intergrowths extensively replacing glaucophane (but leaving fresh winchite) postdate this stage and could potentially belong to the greenschist facies.

## 2.2. Contact Metamorphism

[12] Regional metamorphism is locally overprinted by HT contact metamorphism due to BIC and EM intrusions. Contact metamorphism eventually led to the formation of migmatites in the country rocks (Figures 4a and 4c) and/or pervasively recrystallized the early tectonic foliations, which in some situations were replaced by subhedral to euhedral granoblastic textures (Figures 4f–4h, 4k, and 4l).

## 3. Isotopic Data

[13] In this work we present new isotopic data for EM granodiorites and SN micaschists in order to set landmarks for the most important tectonometamorphic events (Table 2). The K-Ar age determinations were conducted at the Geochronological Research Centre of the University of São Paulo, Brazil, using techniques described by Amaral *et al.* [1966] with modifications. K analyses were by flame photometry with a Micronal B-262 machine, using a lithium internal standard. Ar extraction was made in a high vacuum system with pressure usually less than  $10^{-8}$  mm/Hg. Isotopic analysis of the purified argon was made in MS-1 Nuclide mass spectrometer, now completely modified. All ages were calculated with the decay constants recommended by Steiger and Jager [1977] and are given with standard error ( $1\sigma$ ) estimates. The constants used in the calculations are:  $\lambda\beta = 4.962 \times 10^{-10} \text{ a}^{-1}$ ;  $\lambda\kappa = 0.581 \times 10^{-10} \text{ a}^{-1}$ ; ( $^{40}\text{Ar}/^{36}\text{Ar}$ ) atm = 295.5;  $^{40}\text{K} = 0.01167\% \text{ K}_{\text{total}}$ .

[14] K-Ar analyses were performed on two samples:

[15] 1. Hornblende concentrate from EM granodiorites yields an age of  $318 \pm 11$  Ma. These granodiorites preserve an isotropic texture and intrude the SN micaschists, cutting and metamorphosing the pervasive retrogressive fabric. This means that the host rock was already significantly colder than the granitic magma (Figures 4a and 4b).

[16] 2. Muscovite concentrate from SN micaschists yields an age of  $358 \pm 11$  Ma. These rocks exhibit a microtexture characterized by a pervasive foliation defined

by the coplanar alignment of feldspar and coarse mica grains. The mica (dated muscovite) shows an inclusion pattern of refractory graphite, defining a folded internal foliation (Figures 5 and 6).

[17] Because the EM granodiorite does not show any evidence of postcrystallization transformations, and the closure temperature ( $T_c$ ) for Ar in hornblende is  $450\text{--}500^\circ\text{C}$  [Dodson, 1973], the K-Ar age of circa 318 Ma represents the best estimate of cooling age at  $450\text{--}500^\circ\text{C}$ , which should hence be close to the crystallization age.

[18] The muscovite in the dated micaschist is coarse, clearly visible in hand specimen, mostly millimeter in size. Because there is no evidence for postkinematic recrystallization of the muscovite, this means that the dated micas have not been significantly size reduced by shear or dynamically recrystallized, which is attested by the preservation of earlier deformation patterns inside the grains. Commonly, the analyzed micas show gliding along 001 (Figures 10b and 10e), which has been shown by Reddy and Potts [1999] to not influence  $T_c$ . However, there is some dynamic recrystallization attributed to shearing, with minor neocrystallization of finer grains. This and the coarse grain size could justify the error in the isotopic age. Regarding the meaning of the isotopic age, two critical observations have to be taken into consideration: (1) the temperature of formation of the dated mica should be significantly higher than  $T_c$  for K-Ar in muscovite, because of the observed pervasive recrystallization of K-feldspar and muscovite from previous deformed graphite-rich metasediments, and (2) shearing has not significantly reduced the grain size of muscovite. According to Reddy and Potts [1999], processes in which there is no significant change in grain size are difficult to record true deformation ages. Therefore, we conclude that the isotopic age should represent a cooling age, rather than a deformation age. Since  $T_c$  for Ar in muscovite is  $\sim 350^\circ\text{C}$  [Dunlap *et al.*, 1991], the age of  $358 \pm 11$  Ma can be interpreted as close to the metamorphic peak of the event that affected the metasedimentary rocks. Subsequent shear deformation during exhumation brought the dated rocks to greenschist facies conditions, below  $T_c$  for Ar in muscovite. Isotopic ages from EM and SN are used to constrain different stages of the tectonometamorphic evolution in SW OMZ.

## 4. Structure and Tectonics

[19] In this section we present the key structures, their geometry, sense of shear and metamorphic overprint rela-

**Figure 4.** (a) Igneous contact between EM granodiorites and SN metapelites. (b) Photomicrograph of EM granodiorites exhibiting a coarse grain granoblastic microtexture (fds, feldspar; Hbl, hornblende; Pl, plagioclase) (CPL). (c) Migmatitic layering ( $S_{\text{mig}}$ ) in SN metapelites near the EM intrusives. (d and e) Photomicrograph of quartz-feldspar mylonites in gneisses from SW OMZ (inset shows the mineral stretching lineation  $L_n$  at mesoscopic scale; P-clast, porphyroclast) (CPL). (f to h) Photomicrographs of SW OMZ gneisses, corresponding to thermally recrystallized quartz-feldspar mylonites (S, metamorphic layering overprinting the previous mylonitic foliation; arrow in Figure 4i indicates triple junction) (CPL). (i and j) Photomicrographs of marble mylonites from SW OMZ ( $S_{\text{myl}}$ , mylonitic foliation) (CPL). (k) Photomicrograph of static recrystallized marbles exhibiting granoblastic microtextures near the BIC intrusives (CPL). (l) Marbles showing mesoscopic evidence for posttectonic static recrystallization (random orientated wollastonite fibers, Wo) near EM intrusives.

**Table 2.** Analytical Data Concerning New Isotopic Age Determinations in SW OMZ

SPK	Sample	Concentrate	Rock Type	K (%)	Error K (%)	$^{40}\text{Ar}$ Rad ( $\times 10^{-6}$ cm <sup>3</sup> STP/g)	$^{40}\text{Ar}$ Atm (%)	Age (Ma)	Error Maximum (Ma)
7809	FO-1 OMZ	amphibole	granite	0.6047	0.9326	8.16	27.45	317.8	10.9
7808	FO-2 OMZ	muscovite	micaschist	6.7611	1.6683	103.98	4.70	358.1	11.4

tionships that we subsequently use as basis to establish a chronological sequence of tectonometamorphic events.

#### 4.1. Structures Older Than Circa 358 Ma

[20] Structures of this age must be looked for in rocks that escaped later pervasive deformation and retrogression to greenschist facies: these are typically rocks still recording high-grade metamorphism and/or with minerals refractory to late hydration and retrogression.

##### 4.1.1. Folded Internal Foliation Within Intertectonic Porphyroblasts

[21] The retrogressive planar fabric in SN quartz-feldspar micaschists is mainly defined by the alignment of muscovite, which contours stronger feldspar grains (Figures 5a, 5b, and 6a). Inside these two minerals, an inclusion pattern consisting of a graphite foliation is observed (Figure 5a), which is often folded (Figures 5c–5f) and shows no relationship with the external fabric. These overprint relationships strongly suggest that the graphite internal foliation corresponds to a refractory fabric, recording an early poly-phase tectonometamorphic event testified by the complex fold geometry (Figure 6b, left). This event was followed by thermal recrystallization and growth of feldspar and mica porphyroblasts, preserving the early foliation as an inclusion pattern (Figure 6b, middle). At mesoscopic scale this thermal event was also responsible for the obliteration of the previous deformation, mostly recorded by relict mylonitic/phyllonitic planar-linear fabrics, often only preserved in the form of a metamorphic layering. A later, retrogressive event was responsible for the formation of the external foliation (Figure 6b, right). Following the definition of *Passchier and Trouw* [2005], these mica and feldspar grains can be classified as intertectonic porphyroblasts, formed between two tectonic events: an early one responsible for the formation and folding of the internal foliation (prograde metamorphism?), and a later one responsible for the formation of the retrogressive external foliation. The mica porphyroblasts are dated here at circa 358 Ma, hence the relict graphite fabric must be older, and so does the HP episode associated with a prograde tectonometamorphic evolution, because the mica age is interpreted as a cooling age, indicative of exhumation.

##### 4.1.2. Amphibolite Boudins and Associated Noncylindrical Folds

[22] The early foliation (higher-grade, mylonitic, see Figures 4d, 4e, 4i, and 4j) is often associated with boudinage-folding processes studied in detail by *Marques and Cobbold* [1995] and *Rosas et al.* [2001, 2002], which typically occur in marbles (Figure 7). The structures consist mainly of noncylindrical folds (including sheath folds) distributed around rigid inclusions (presently amphibolites in the broad sense), corresponding to mesoscopic quarter structures from which top to south shear sense can be deduced (Figure 7). The trails of mafic boudins do not cut the mylonitic foliation in the marbles; instead they are contoured by the foliation. However, the early foliation is cut by apophyses born in the BIC (Figure 8). This shows that both the mylonitic fabric and the boudinage-folding patterns have formed simultaneously, under top to south shearing, before the intrusion of the BIC (circa 340–350 Ma [*Dallmeyer et al.*, 1993; *Pin et al.*, 1999]) (Table 1 and Figure 9).

##### 4.1.3. Boudins of HP Metamorphic Rocks

[23] In some locations, the mafic bodies observed within marbles and SN micaschists have escaped complete retrogression, and the HP metamorphic parageneses can still be recognized (see map of Figure 2). In contrast, the weaker host rocks are pervasively affected by later shearing, hydration and retrogression to low-amphibolite/greenschist facies. This means that the prograde HP metamorphism recorded by the mafic boudins occurred prior to generalized retrogression during exhumation. Taking into account that: (1) sediments with embedded mafic rocks were subducted to great depths, (2) subduction was to the north [e.g., *Ribeiro et al.*, 1979; *Martinez and Ibaruchi*, 1983; *Santos et al.*, 1987, 1990; *Quesada et al.*, 1994], and (3) surface and geophysical soundings show structural features and reflectors dipping to the north, we conclude that southward shearing and the concomitant boudinage correspond to thrusting synthetic with the northward subduction (underthrusting) beneath the OMZ margin. Therefore, the HP metamorphism must have occurred during this deformation, prior to circa 358 Ma, which corresponds to the mica cooling age in the host metapelites, indicative of retrogression and exhumation.

**Figure 5.** SN quartz-feldspar micaschists: (a) (left) Graphite folded internal foliation (graph-Si) preserved inside feldspar (fds) and mica (mic) grains; (right) detail of the internal foliation (graph-Si) continuously crossing through the boundary between feldspar and mica grains. Note that both these minerals are overgrowing the refractory graphite inclusion pattern (CPL). (b) Deflection of mica around a feldspar grain (CPL). (c and d) Microboudins of feldspar bearing a folded graphite internal foliation (Figure 5d, left, plain polarized light, and Figure 5d, right, cross polarized light). Note that direction of boudinage (white arrows) is parallel to the mica grains defining the external foliation (Se). (e) Internal foliation preserved inside feldspar and mica grains exhibiting a crenulation cleavage (S-foliation domain; m-microlithons) (CPL). (f) Mimetic growth of mica over the crenulated graphite refractory fabric (Si) in the rock matrix; and inside a feldspar grain (fds) (CPL).

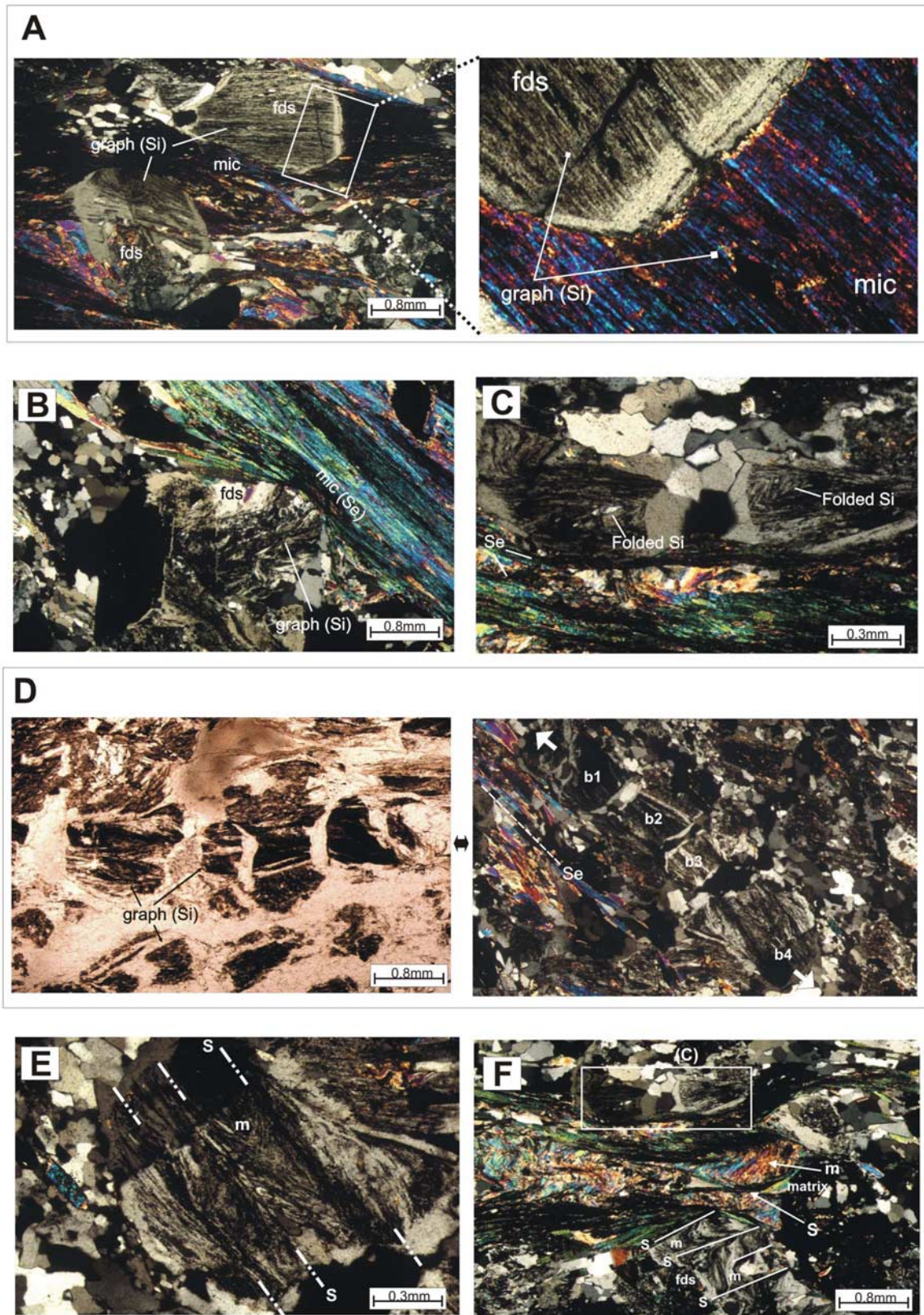
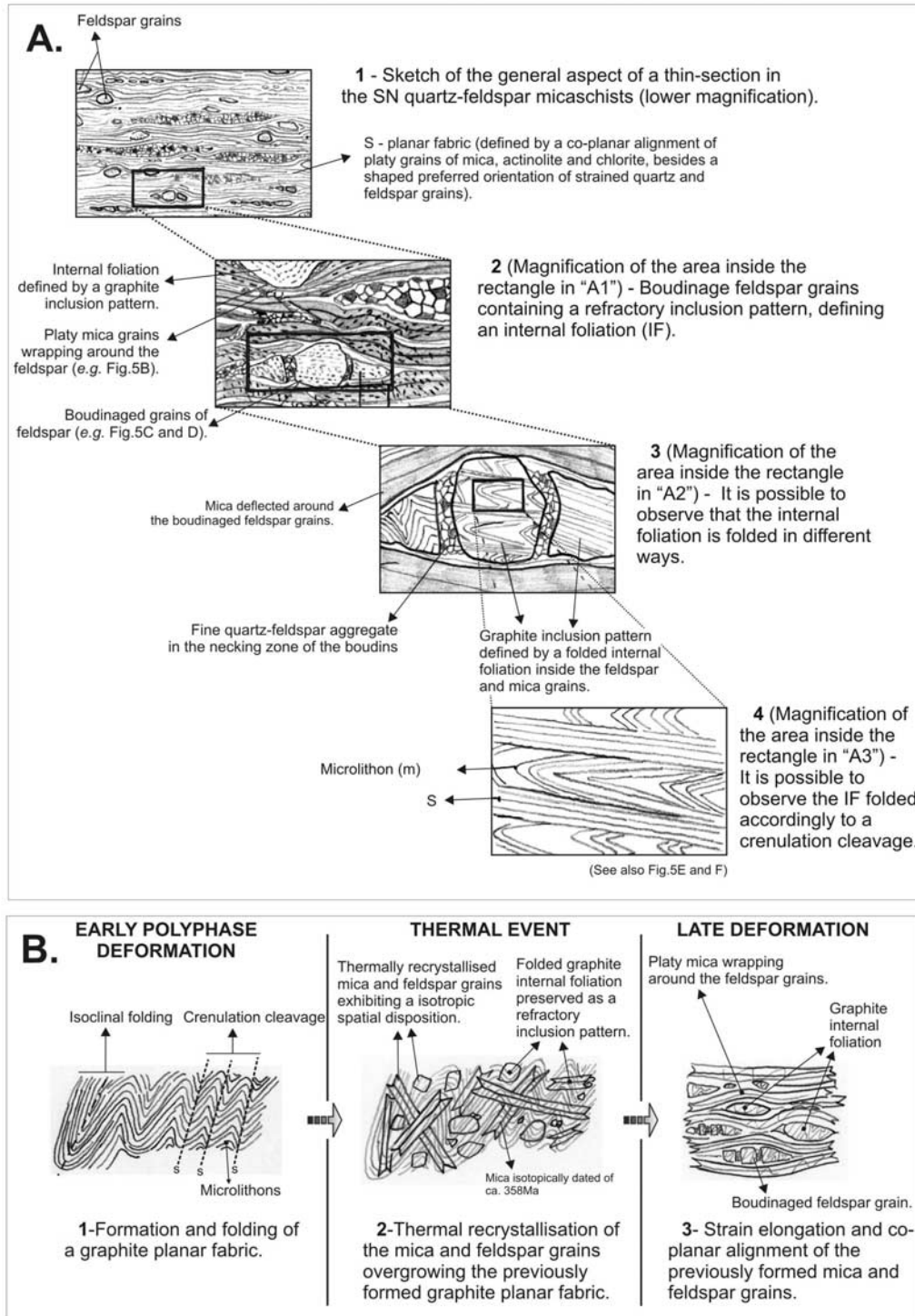


Figure 5



**Figure 6.** (a) Schematic zooming through the main different microstructures and microtextural overprint relationships, observable at different scales in the SN quartz-feldspar micaschists. (b) Interpreted chronologic sequence of events responsible for the presently observed microtexture.

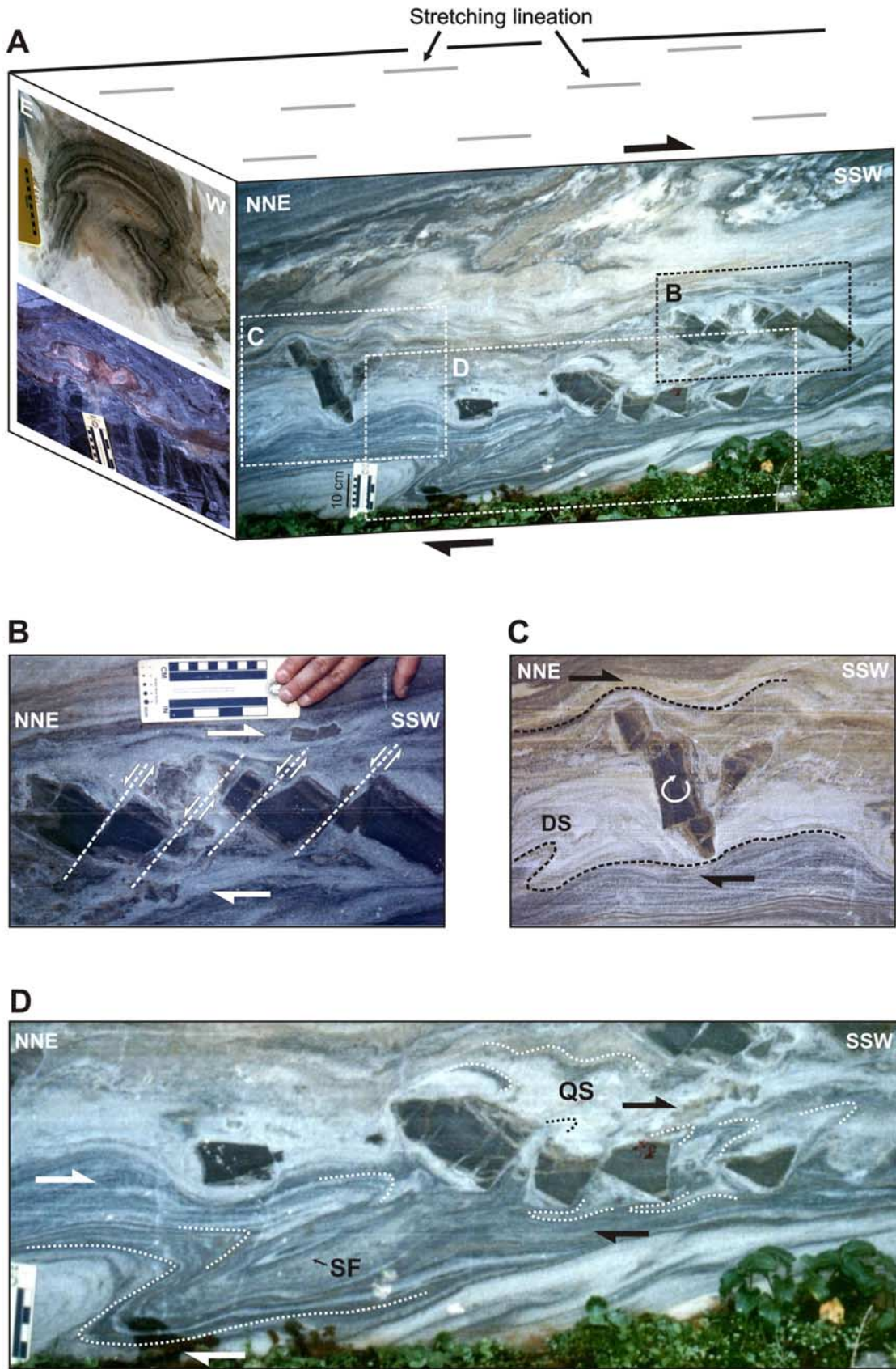


Figure 7

## 4.2. Structures Between Circa 358 and Circa 318 Ma

### 4.2.1. Phyllonitic Planar-Linear Fabric

[24] The foliation defined by mica in SN micaschists formed under low-amphibolite to greenschist facies conditions, and corresponds to the main tectonic planar fabric that affects the rocks in the detachment zone within SW OMZ (see Figure 2b). This foliation corresponds to a micaceous mylonite, or phyllonite as defined by *Passchier and Trouw* [2005]; it dips, in average, gently to the northeast, and includes a stretching lineation plunging variably between NNW and NNE. The northeastward dip of this pervasive foliation and related shear zones can be depicted from the deep seismic profile presented by *Simancas et al.* [2003] and from Figure 2b. Only locally and close to the BIC, the foliation strikes closer to N-S (in Serpa and Alvito structures, Figure 2a).

[25] The age span of the retrogressive mylonitic foliation is yet not fully constrained because (1) the age of the mica defining the phyllonitic foliation in SN is interpreted as a cooling age, rather than a deformation age and (2) deformation may have started at a temperature above  $T_c$  and certainly proceeded after  $T_c$  was crossed during exhumation. Therefore, the age depends on the duration and metamorphic evolution during the exhumation stage. However, the upper age must always be older than 318 Ma because the phyllonitic foliation is affected by the EM intrusion at circa 318 Ma.

### 4.2.2. Shear Sense Indicators

[26] Sections cut perpendicular to the phyllonitic foliation and parallel to the stretching lineation show a variety of classical shear sense criteria, from which consistent top to north shear sense has been deduced (Figure 10). This is in agreement with all previous publications on the SW OMZ [e.g., *Fonseca and Ribeiro*, 1993; *Quesada et al.*, 1994; *Fonseca et al.*, 1999; *Silva and Pereira*, 2004; *Araújo et al.*, 2005]. The used indicators are  $\delta$  and  $\sigma$  clasts, including mica fish and bookshelf sliding, C-S foliations, C-C' associations (Figures 10a–10c and 10e), and garnet porphyroblasts with internal sigmoidal to spiral foliations (Si) defined by mineral inclusions of quartz, calcite, and opaque minerals (Figures 10d, 10g, and 10h).

## 4.3. Structures Syn- to Post-Circa 318 Ma

[27] The EM granodioritic rocks postdate all pre-Mesozoic penetrative ductile deformation, because they always exhibit an isotropic texture (see Figures 4a and 4b) and are only affected by late Variscan fracturing [*Marques et al.*, 2002]. Close to the EM, the host SN rocks are commonly transformed into migmatites, through partial melting and compositional segregation into alternating quartz and feldspar-rich leucocratic layers, and mica and amphibole-rich melanocratic layers (Figure 4c). The migmatites formed

from country rock phyllonites, as a consequence of contact metamorphism, and show no postrecrystallization deformation. Therefore, the tectonometamorphic event that originated the phyllonites in the country rock must be older than the EM (circa 318 Ma). Similarly, the marbles close to the EM were also subjected to static recrystallization recorded by very coarse-grained isotropic textures (Figures 4k and 4l).

## 5. Chronology of Tectonometamorphic Events

[28] On the basis of the structural and metamorphic overprint relationships presented above, we summarize the chronological sequence of the main pre-Mesozoic tectonometamorphic events (TM) in SW OMZ (Figure 11).

### 5.1. $TM_n$ : Subduction-Related HP Metamorphism and Southward Shearing (More Than Circa 358 Ma)

[29] The oldest tectonometamorphic event recognized is the prograde HP metamorphism preserved in blueschists and eclogites. The reconstruction of the history that followed the HP event is not straightforward because subsequent pervasive retrogression under greenschist facies conditions erased the older tectonometamorphic evolution almost completely. However, some mesoscale and microscale structures may be related with the higher-grade tectonometamorphic evolution. This is the case of the relict graphite fabric found in SN micaschists and of the noncoaxial structures corresponding to the boudinaged-folding patterns observed mostly in the marbles, which indicate transport with top to SSW consistent with subduction toward the north.

[30] Different PT conditions between eclogites, blueschists and some amphibolites, presently very close, may only reflect evolution during the same tectonometamorphic event, although at different lithospheric levels, now brought together by exhumation.

### 5.2. $TM_{n+1}$ : HT Recrystallization (More Than 358 Ma Ago)

[31] In SN micaschists, this thermal event was responsible for the almost complete recrystallization of an original texture, with growth of mica and feldspar porphyroblasts over a relict fabric recorded by refractory graphite grains. These still preserve a folded internal foliation, which indicates that this foliation was formed and subsequently folded during an earlier tectonometamorphic event.

### 5.3. $TM_{n+2}$ : Northward Retrogressive Shearing (Circa 358 Ma and More Than Circa 318 Ma)

[32] A shearing event followed HT recrystallization, developing a phyllonitic foliation under low amphibolite to greenschist facies conditions. This foliation dips to north,

**Figure 7.** (a) Schematic block diagram illustrating the boudinage-folding pattern observed in the SW OMZ marbles. The planar fabric is deflected and folded around the boudins following *Rosas et al.* [2001, 2002]. Sheath folds (SF) “eye” patterns are observed associated with the trails of mafic boudins along NNE-SSW vertical sections. “Mushroom” patterns of this same type of folds are preferably observed along E-W sections. Top and bottom black arrows indicate sense of shear. (b) Detail of bookshelf boudinage pattern inside the ductile sheared marbles. (c) Detail of rotated (upright) boudin showing associated drag sheath folds (DS). (d) General aspect of the boudinage-folding pattern quarter structures (QS).

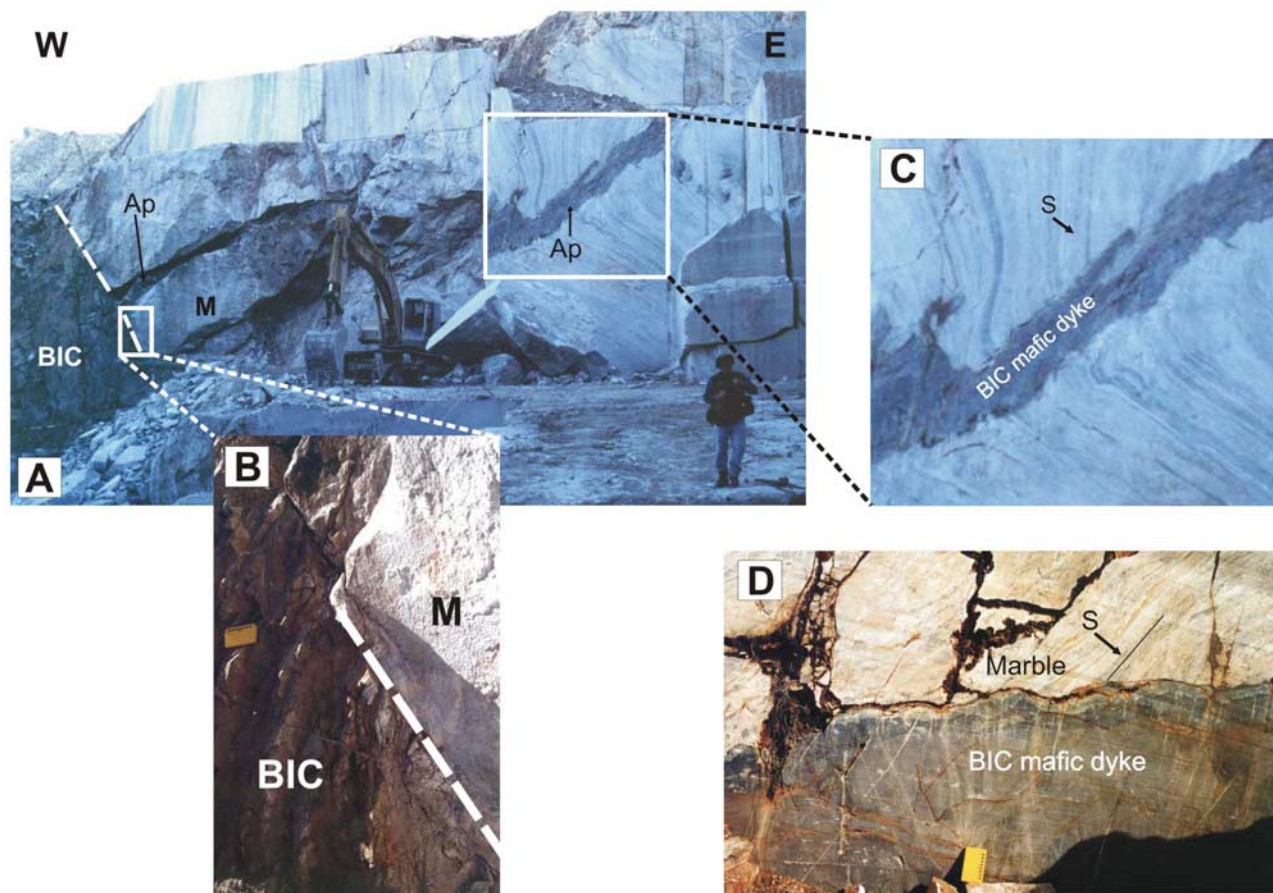


**Figure 8.** (a) Outcropping igneous contacts between BIC and marbles (M) and between BIC diorite apophyses (Ap) intruding marbles and cutting the planar fabric (S). (b) Detail of contact between BIC and marbles in Figure 8a. (c) Detail of contact between BIC diorite Ap intruding marbles and cutting S in Figure 8a. (d) BIC diorite dyke cutting the S planar fabric in marbles.

which associated with top to north sense of shear makes the shear zones ductile normal faults. The zone comprising the north dipping and top to north shearing is here defined as the detachment zone responsible for exhumation of deep seated rocks by inversion of the earlier, subduction-related, thrusts (see Figure 2b).

#### 5.4. $TM_{n+3}$ : Static Recrystallization and Migmatism (Circa 318 Ma)

[33] A new HT episode imposed posttectonic static recrystallization in the country rock units near the contact with EM, locally erasing most of the previously developed tectonic fabrics.

### 6. Geodynamic Evolution of the SW Iberian Variscan Orogen: Discussion

[34] The geodynamic evolution of the SW OMZ has been described in the literature according to four main hypotheses: (1) subduction and synthetic accretion, (2) flake tectonics, (3) transcurrent tectonics, and (4) ridge subduction tectonics. These hypotheses do not take into account

postcollisional orogenic collapse, despite what has been described for other areas of the Variscan orogen [e.g., *Ménard and Molnar*, 1988; *Matte*, 1991; *Malavieille*, 1993; *Burg et al.*, 1994]. We propose a new interpretation that incorporates subduction of segments of a continental margin and subsequent postorogenic collapse and exhumation.

[35] *Bard et al.* [1973], *Matte* [1986, 1991] and *Simancas et al.* [2003, 2005] have described the tectonic evolution of the Iberian Variscides as a classical orogenic belt, involving northward subduction and synthetic southward thrusting; however, the exhumation mechanisms of the HP metamorphic rocks have not been addressed or explained.

[36] Several authors have suggested northward obduction of an oceanic crust simultaneous with northward subduction beneath the SW OMZ margin [*Ribeiro and Pereira*, 1986; *Fonseca and Ribeiro*, 1993; *Quesada et al.*, 1994; *Fonseca et al.*, 1993, 1999; *Ribeiro et al.*, 2007]. They consider the HP metamorphic peak conditions to be associated with top to north sense of shear.

[37] *Silva and Pereira* [2004] favor the idea of an orogen-parallel transcurrent deformation diachronically affecting the whole of the OMZ, through alternating left-lateral transtension and transpression. This deformation would be

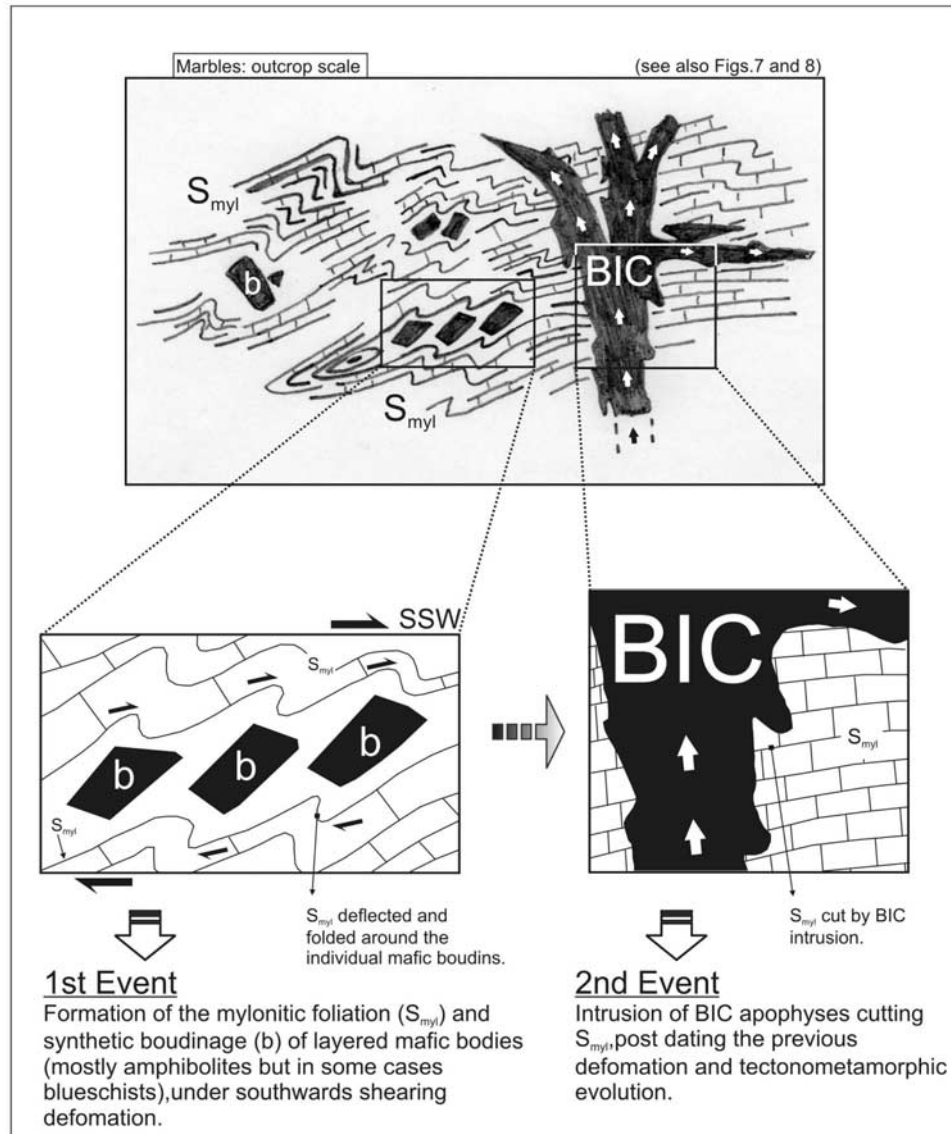


**Figure 9.** Schematic illustration of pre-BIC structural overprint relationships, and deduced partial chronological succession of tectonometamorphic events.

responsible for the diachronic syntectonic opening and closure of several regional basins, among which the one where the BAOC rocks would have originated. This hypothesis does not take into account oceanic subduction. Bard [1977, 1992] also did not favor subduction of oceanic crust, and rejected the hypothesis of ophiolite obduction. Bard [1992] suggested fast continental rifting in the Silurian followed by continental subduction.

[38] The main tectonometamorphic features characterizing the Aracena Metamorphic Belt (AMB) [e.g., Bard, 1977; Bard and Moine, 1979; Crespo-Blanc, 1987; Crespo-Blanc and Orozco, 1988; Castro et al., 1996, 1999; Díaz Azpiroz et al., 2006] in the eastern domains of the SW Iberian Variscan suture (see Figure 1b) are noticeably different from the ones described in the present work for the western segment, namely in the following:

**Figure 10.** (a) Photomicrographs of SN micaschists showing micro  $C'$  and  $C+S$  shear bands, polycrystalline foliation fish and micafish. (b) Micafish (zoomed from A) exhibiting microbookshelf sliding along mica cleavage planes. (c) Micro  $C+S$  shear bands in XM greenschists. (d) The  $\delta$  clast indicating top to right sense of shear in XM greenschists. (e) Micafish exhibiting microbookshelf sliding along mica cleavage planes and  $\sigma$  geometry of tails indicating top to right sense of shear. (g and h) garnet porphyroblasts showing sigmoidal to spiral inclusion patterns. CPL in all photomicrographs. Arrows indicate deduced sense of shear in all cases (Grt, garnet; Si, internal foliation (inclusion pattern); Se, matrix external foliation; SS, strain shadow; SC, strain cap).

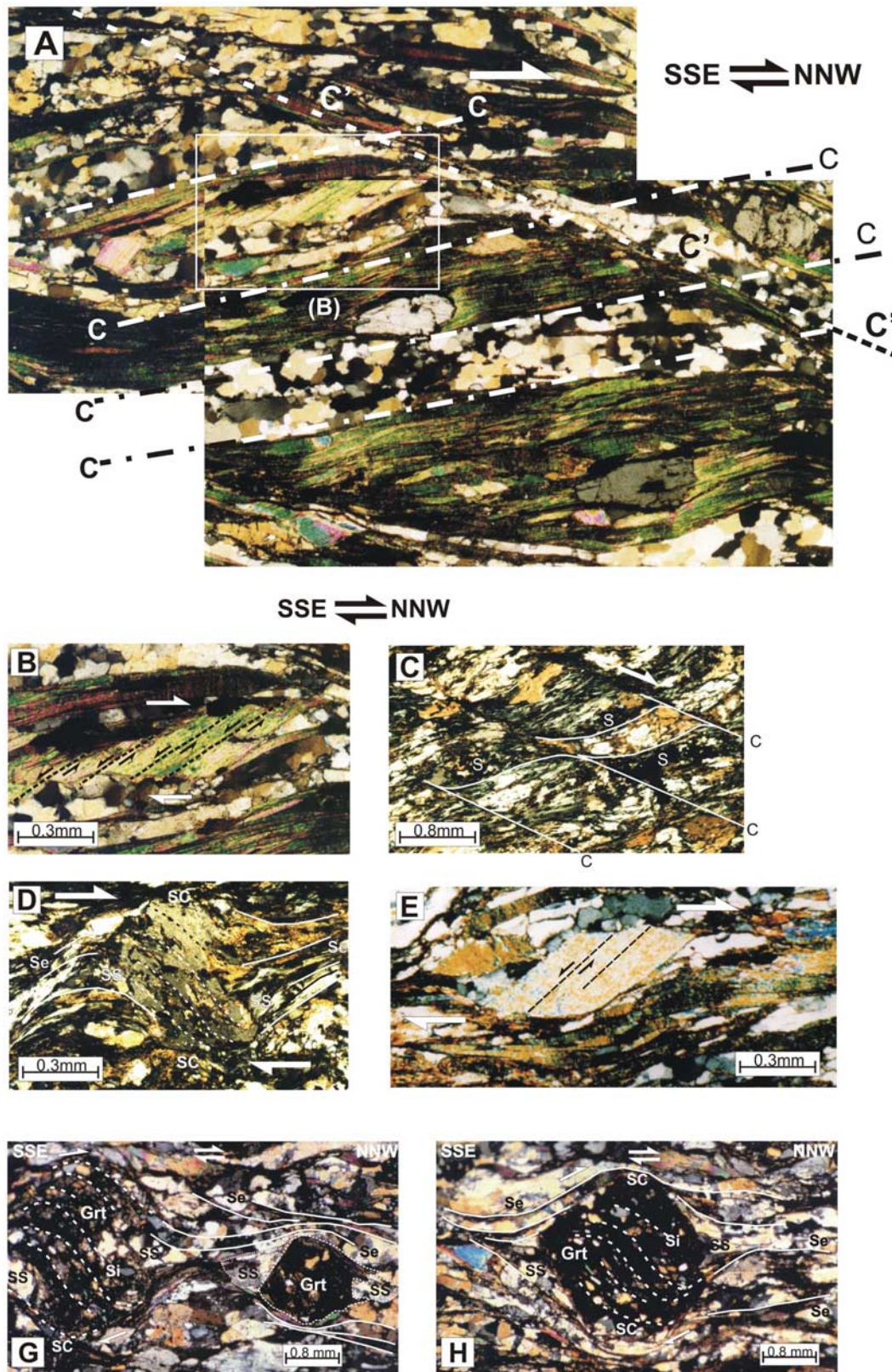


Figure 10

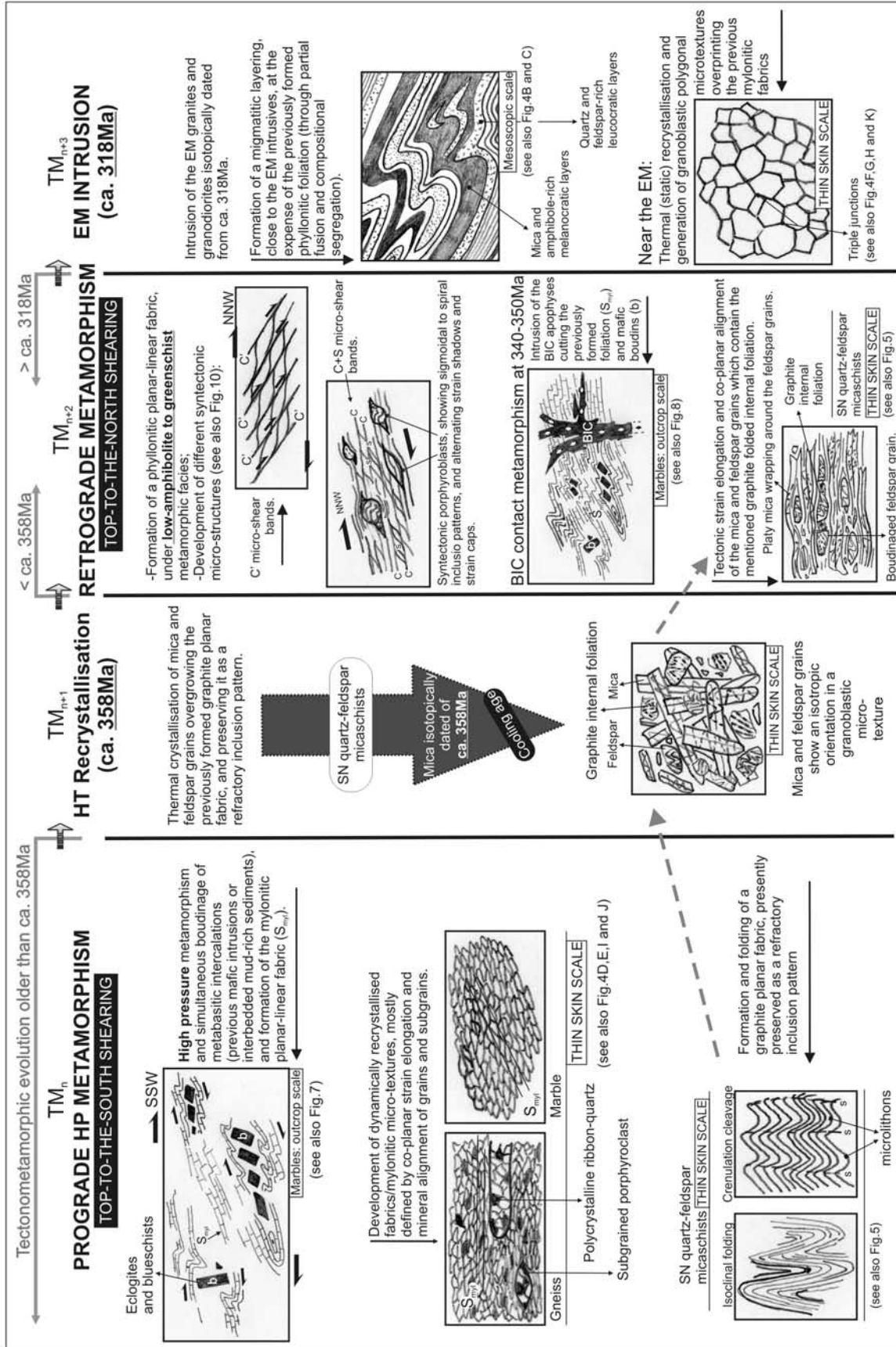
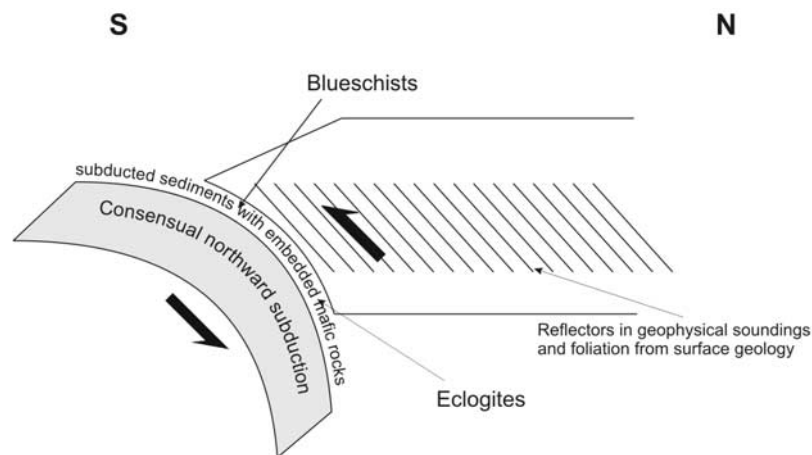


Figure 11. Proposed chronological sequence of tectonometamorphic events for the SW OMZ.



**Figure 12.** Schematic summary of the critical data sustaining the presently proposed interpretation for the geodynamic evolution of the SW Iberian Variscides.

[39] 1. The OD rocks in the eastern segment show an inverted metamorphic gradient, higher in its upper levels (granulite facies) and lower at the base (amphibolite to greenschist).

[40] 2. In the east, the peak (main) metamorphic event recorded in rocks from both the oceanic (OD) and the continental (CD) domains is HT/LP. This metamorphic event is dated at circa 380–370 Ma in the CD [Dallmeyer and Quesada, 1992; Díaz Azpiroz *et al.*, 2006]. In the west, the peak is HP/LT and older than circa 358 Ma.

[41] 3. According to Castro *et al.* [1999], the cooling ages of oceanic amphibolites decrease from west (circa 343 Ma) to east (circa 328 Ma).

[42] 4. In the east the deformation affecting both the OD and CD is generally top to south shearing, although in some cases top to north shearing in the CD has also been reported. In the west, the most common deformation is top to north shearing. The interpretation by Castro *et al.* [1996, 1999] and Díaz Azpiroz *et al.* [2006] considers the subduction of a ridge underneath the OMZ continental margin, responsible for the isobaric heating of the overriding CD and for the production of boninitic magmas in the lithospheric wedge. The continuation of subduction would have put in contact the heated CD with the underlying oceanic crust of the OD, which would have been heated in this way from its structural top. This would account for the inversion of the metamorphic gradient in the OD, and would also be responsible for the relaxation of the compressive stress regime at the upper plate, with crustal extension in the CD caused by isobaric heating. According to this hypothesis, the structures associated with top to north shearing in the CD would thus be formed between contraction events, recording extensional collapse caused by short-termed thermal relaxation.

[43] In western OMZ, the reported evidence of an HP metamorphic event shows that subduction must be considered as a major step in the Variscan geodynamic evolution. However, no previous work focusing on the SW Iberian suture has addressed or explained the crucial issue that is the exhumation of the HP rocks and their present-day structural

position. In the east, the top to south shearing is interpreted as the result of northward subduction, whereas in the West it had not been recognized prior to the present work. In the west, the top to north shearing is clearly retrogressive and pervasively affects the rocks comprising this segment of the suture.

[44] Our interpretation takes into consideration new and previous data to show subduction of a continental margin and continental collision, top to south shearing contemporaneous with subduction, postorogenic collapse and exhumation, and to set an upper age to the Variscan eclogite facies. The critical data that serve as ground for our hypothesis are (Figure 12) (1) subduction toward the north (so far undisputed), (2) structural features and reflectors dipping to north, as shown by surface geology and geophysical soundings [Monteiro Santos *et al.*, 1999; Almeida *et al.*, 2001; Monteiro Santos *et al.*, 2002; Simancas *et al.*, 2003; Pous *et al.*, 2004], (3) subduction of continental margin sediments with embedded mafic rocks (carbonates with blueschists inside), (4) opposite senses of shear, of different age, associated with the structures developed either during early HP prograde tectonometamorphic events (top to south shearing,  $TM_n$ ) or during later retrogression (top to north shearing,  $TM_{n+2}$ ), respectively (see Figure 2b), (5) present occurrence of HP rocks at the surface, and (6) along-strike variations in metamorphic record. We propose a simpler way of explaining the exhumation of the HP metamorphic rocks, and of unifying observations along the western and eastern segments of the SW Iberian Variscan suture, and (7) extension in the neighboring South Portuguese Terrane with formation of a wide and deep basin between circa 365 and 310 Ma, filled with sediments eroded from the OMZ, and with volcanics. Our interpretation incorporates previously proposed ideas for the whole of the Variscan belt in Western Europe, it follows published interpretations for the evolution of the Caledonides in western Norway [e.g., Norton, 1986; Andersen and Jamtveit, 1990; Andersen *et al.*, 1991], which include the exhumation of UHP rocks, and for the Himalaya-Tibet [Chemenda *et al.*, 2000; Boutelier *et al.*, 2003], and it

follows *Ring et al.* [1999] in their idea that extension (normal faulting) and denudation combine to exhume deep seated rocks efficiently.

[45] The present hypothesis comprises the stages in sections 6.1–6.4:

### 6.1. Passive Margin Stage

[46] Lower Cambrian continental rifting stage, responsible for the thinning of the precursor OMZ continental crust [e.g., *Ribeiro et al.*, 1990; *Quesada*, 1990, 1991, 1992; *Quesada et al.*, 1994; *Fonseca et al.*, 1999]. Subsequent formation of the Rheic Ocean was followed by a Cambrian–Silurian passive margin stage.

### 6.2. Early Subduction/Compressional Stage

[47] This stage is characterized by oblique subduction of the Rheic oceanic slab beneath the SW OMZ margin, by compression in the overriding plate, by subduction erosion and burial of continental segments of the margin, and by HP metamorphism (TM<sub>n</sub> event, recorded by blueschists and mafic eclogites within marbles and SN metapellites, respectively). The structures formed during this northward subduction stage are associated with southward directed transport, because structural features and reflectors systematically dip to the north. As indicated by the new data reported in this paper, this subduction/compressional stage must be prior to 358 Ma.

### 6.3. Postorogenic Collapse, Extension, and Exhumation of HP Rocks

[48] At this stage effective convergence (compression in the overriding plate) ends, thus horizontal forces cannot support the mountain belt any longer and it begins to collapse. Effective convergence can cease in two typical ways: by continental collision followed by cessation of subduction, or by transformation of roll-forth into roll-back subduction (continuous subduction). Both can set off thermal reequilibration through isotherm recovery in the thickened lithosphere, triggering melting near the suture and producing the BIC magmatism sometime prior to circa 350 Ma. The circa 340 Ma <sup>40</sup>Ar/<sup>39</sup>Ar cooling age means that the BIC was being exhumed at this stage. Thermal relaxation is concomitant with postorogenic extension, through inversion of earlier major underthrusts related to subduction, changing shear sense and exhuming HP rocks. This is supported by the reported evidence of top to north sense of shear in retrogressive metamorphic conditions. Shear sense to north and main shear zones and foliation dipping to north, as shown by large-scale surface and geophysical data, makes shear zones normal faults. Therefore, they should be related to an extensional episode. Top to north and north dipping shear-related structures define a zone of detachment (see Figure 2b) that exhumed the negatively buoyant metasediments with embedded blueschists and eclogites. Because it is the latest ductile deformation and lowest grade (accompanying retrogression), we interpret it as postorogenic collapse. Extension must have stopped in greenschist facies conditions because that is the lowest grade in the deformed rocks affected by

shearing to north. The Alpine deformation is much attenuated in this region hence the Meso–Cenozoic uplift should not exceed 1 to 2 km. Therefore, isostatic rebound and denudation following extension brought the light roots of the mountain belt to very shallow levels.

[49] Lithospheric extension and exhumation is also recorded in the neighboring terrane to the south. The South Portuguese Terrane (SPT) comprises, from bottom to top [e.g., *Mac Gillavry*, 1961; *Schermerhorn*, 1971], as follows:

[50] 1. Shallow platform sediments are interlayered shales and quartzites with limestones on the top comprising the Phyllite-Quartzite Formation of the Pyrite Belt Domain, with top limestones dated circa 365 Ma and unknown base. These deposits show that a stable shallow platform existed sometime prior to 365 Ma ago in the SPT, which means that there was no significant tectonic activity nearby to perturb the system. A volcano-sedimentary complex conformably overlies this formation.

[51] 2. Volcano-sedimentary deposits are bimodal volcanics and interfingering siliciclastic sediments comprising the Volcano-Sedimentary Complex of the Iberian Pyrite Belt, ranging in age between circa 365 and 335 Ma. These deposits indicate that the platform in NE SPT evolved into a lithospheric-scale rift recorded by bimodal volcanism in the Pyrite Belt Domain, with development of crustal-scale basins/grabens where the volcano-sedimentary complex was deposited. A flysch deposit conformably overlies this complex.

[52] 3. Flysch deposits are thick flysch sequences with age ranging from circa 335 to 310 Ma old, were deposited in a strongly subsiding basin. *Mac Gillavry* [1961] and *Schermerhorn* [1971] have concluded that the origin of the detritus comprising the flysch had to be to the north, in the OMZ (which they called the Beja Geanticline). Therefore, topographic relief built up outside and to the north of the SPT during extension. Moreover, remobilised fossils from the youngest flysch vary in age between circa 540 and 410 Ma [*Pereira*, 1999]. This indicates that the fossils came from outside the SPT, because rocks of those ages are not known to crop out in the SPT.

[53] It is clear from data in the SPT that (1) extensional tectonics took place between circa 365 Ma and 310 Ma ago, because this is the age of the sediments deposited in the opening and deepening SPT trough bordering the OMZ to the south, and (2) the detritus filling the SPT basin were eroded from an uplifting OMZ. Denudation in the OMZ must have been considerable to account for the great amount of detritus deposit in the SPT trough. The continuous supply of OMZ derived detritus to the flysch in the SPT shows that exhumation and denudation in OMZ was very active between circa 335 to 310 Ma ago. Regarding the OMZ immediately to the north, the existing <sup>40</sup>Ar/<sup>39</sup>Ar cooling ages on amphiboles show that the OMZ rocks were being uplifted in the same time interval, although earlier in the west (circa 343 Ma) than in the east (circa 328 Ma) [*Dallmeyer and Quesada*, 1992; *Castro et al.*, 1999]. Putting together extension, origin of detritus, uplift, and age of deformation in the two neighboring terranes, we conclude that extension was occurring contemporaneously

in both terranes. In the thickened OMZ, exhumation and denudation took place by normal faulting, as shown by the present data. Uplift and denudation of the OMZ seems to have continued until circa 310 Ma ago, the age of the youngest flysch fed by sediments derived from the OMZ.

[54] A new compressional event started around 310 Ma ago, which heavily deformed the rocks in the SPT and reactivated the contact between the SPT and the OMZ as a thrust. The oldest sediments in the SPT set an age limit to the initiation of extension, and hence a limit between compressional and subsequent extensional tectonics, which is around 365 Ma. The early compressional tectonics can still be recognized in the OMZ, as shown here for west OMZ, but cannot be observed in the SPT because rocks older than circa 365 Ma are not known to crop out in this terrane. The youngest flysch sets a limit to the tectonic deformation of the SPT under compression, and thus a limit between extensional and subsequent compressional tectonics, which is circa 310 Ma. This late compression can result from roll-back subduction changing to roll-forth subduction. If the compressional/extensional/compressional tectonic succession is envisaged as the result of flipping between roll-forth and roll-back subduction, this means that subduction to the north was continuous throughout the Variscan. Continued subduction of the Rheic to the north eventually led to subduction-related magmatism recorded in tholeiitic, calc-alkaline and shoshonitic bodies in SW OMZ [Santos *et al.*, 1987, 1990]. These volcano-sedimentary complexes were dated between circa 350 and 330 Ma by Pereira *et al.* [2006].

#### 6.4. Final Thermal Reequilibration and Isostatic Rebound

[55] At this stage, continuation of isotherm reequilibration and rise in the lithosphere is more widespread, affecting

the light roots of the orogen, and promoting the EM postkinematic magmatism (TM<sub>n+4</sub>), dated in the present paper at circa 318 Ma. As isostatic rebound came to an end, earlier shallow structures were removed by denudation, and dipping of earlier or inverted thrusts decreased significantly.

[56] Our interpretation does not exclude the “ridge subduction hypothesis”; on the contrary, complements it with new data along strike to the west. Subduction of hot, lighter rocks of an ocean ridge in the east could be responsible for low dipping subduction as presently recognized in part of the southern Andes. As a consequence, (1) metamorphic grade is likely to be of higher temperature, as in the case of the AMB to the east, (2) HP metamorphism (blueschists and eclogites) is unlikely to occur in the east because of the higher temperature of subducted rocks (HP rocks have never been found to the east), and (3) postorogenic collapse and isostatic rebound should be attenuated relatively to the western sector, because mountain roots should be shallower. This could justify the predominance of the compressive (orogenic related) top to south shearing in the east. On the other hand, blueschists and eclogites (HP metamorphism) in the west point to steeper subduction and possible deeper roots of the mountain belt. This would promote more vigorous postorogenic extension and isostatic rebound that would justify the predominance of the inversion-related and retrogressive top to north shearing and the older cooling ages in the west.

[57] **Acknowledgments.** We thank P. D. Ryan, A. Crespo-Blanc, and Onno Oncken for constructive reviews and editorial work that helped improve the manuscript. F. Rosas acknowledges a Ph.D. scholarship (PRAXIS XXI/BD/9220/96) of Fundação para a Ciência e Tecnologia (FCT). This is a contribution to research project TEAMINT (POCTI/CTE/48137/2002). R. Caranova is acknowledged for help in figure production.

## References

- Almeida, E. P., J. Pous, F. A. Monteiro Santos, P. Fonseca, A. Marcellino, P. Queralt, M. R. Nolasco, and L. A. Mendes-Victor (2001), Electromagnetic imaging of a transpressional tectonic in SW Iberia, *Geophys. Res. Lett.*, *28*(3), 439–442, doi:10.1029/2000GL012037.
- Amaral, G., U. G. Cordani, K. Kawashita, and J. H. Reynolds (1966), Potassium-argon dates of basaltic rocks from Southern Brazil, *Geochim. Cosmochim. Acta*, *30*, 159–189, doi:10.1016/0016-7037(66)90105-0.
- Andersen, T. B., and B. Jamtveit (1990), Uplift of deep crust during orogenic extensional collapse: A model based on field studies in the Sogn-Sunnfjord region of western Norway, *Tectonics*, *9*, 1097–1111, doi:10.1029/TC009i005p1097.
- Andersen, T. B., B. Jamtveit, J. F. Dewey, and E. Swenson (1991), Subduction and exhumation of continental crust; major mechanisms during continent-continent collision and orogenic extensional collapse, *Terra Nova*, *3*, 303–310, doi:10.1111/j.1365-3121.1991.tb00148.x.
- Araújo, A., P. Fonseca, J. Munhá, P. Moita, J. Pedro, and A. Ribeiro (2005), The Moura Phyllonitic Complex: An accretionary complex related with obduction in southern Iberia Variscan Suture, *Geodin. Acta*, *18*(5), 375–388, doi:10.3166/ga.18.375-388.
- Bard, J. P. (1977), Signification tectonique des métatholeiites d’affinité abyssale de la ceinture métamorphique de basse pression d’Aracena (Huelva, Espagne), *Bull. Soc. Geol. Fr.*, *XIX*(2), 385–393.
- Bard, J. P. (1992), Les complexes intrusifs acide-basique calco-alcalins de la chaîne varisque sud-ibérique et leurs liaisons avec les grands cisaillements transpressifs de Badajoz-Cordue et de la zone sud-ibérique: Proposition de modèles géodynamiques impliquant des processus de subduction continentale, *C. R. Acad. Sci.*, *314*, 711–716.
- Bard, J. P., and B. Moine (1979), Acebuches amphibolites in the Aracena hercynian metamorphic belt (southwest Spain): Geochemical variations and basaltic affinities, *Lithos*, *12*, 271–282, doi:10.1016/0024-4937(79)90018-5.
- Bard, J. P., R. Capdevilla, P. Matte, and A. Ribeiro (1973), Geotectonic model for the Iberian Variscan Orogen, *Nature Phys. Sci.*, *241*, 50–52.
- Boutelier, D., A. Chemenda, and J.-P. Burg (2003), Subduction versus accretion of intra-oceanic volcanic arcs: Insight from thermo-mechanical analogue experiments, *Earth Planet. Sci. Lett.*, *212*, 31–45, doi:10.1016/S0012-821X(03)00239-5.
- Brun, J. P., and J.-P. Burg (1982), Combined thrusting and wrenching in the Ibero-Armorican arc: A corner effect during continental collision, *Earth Planet. Sci. Lett.*, *61*, 319–332, doi:10.1016/0012-821X(82)90063-2.
- Burg, J. P., P. Bale, J. P. Brun, and J. Girardeau (1987), Stretching lineation and transport direction in the Ibero-Armorican arc during the Siluro-Devonian collision, *Geodin. Acta*, *1*, 71–87.
- Burg, J. P., J. Van den Driessche, and J. P. Brun (1994), Syn- to post-thickening extension in the Variscan belt of western Europe: Modes and structural consequences, *Geol. Fr.*, *3*, 33–51.
- Carvalhosa, A. B. (1965), Contribuição para o conhecimento geológico da região entre Portel e Ficalho, *Mem. Serv. Geol. Portugal*, *11*, 132.
- Carvalhosa, A. B. (1972), Estudo geológico-petrográfico da região de Viana do Alentejo-Alvito, *Bol. Soc. Geol. Portugal*, *18*, 7–56.
- Carvalhosa, A. B. (1983), Esquema geológico do Maciço de Évora, *Comun. Serv. Geol. Portugal*, *69*, 201–208.
- Carvalhosa, A. B., and G. Zbyszewski (1991), Carta geológica de Portugal à escala 1/50000, Folha 40-C, Serv. Geol. de Portugal, Lisbon.
- Castro, A., C. Fernandez, J. D. de la Rosa, I. Moreno-Ventas, and G. Graeme Rogers (1996), Significance of MORB-derived amphibolites from the Aracena Metamorphic Belt, southwest Spain, *J. Petrol.*, *37*, 235–260, doi:10.1093/petrology/37.2.235.
- Castro, A., C. Fernández, H. El-Hmidi, M. El-Biad, M. Díaz Azpiroz, J. D. de la Rosa, and F. Stuart

- (1999), Age constraints to the relationships between magmatism, metamorphism and tectonism in the Aracena metamorphic belt, southern Spain, *Int. J. Earth Sci.*, 88, 26–37, doi:10.1007/s005310050243.
- Chemenda, A. I., J.-P. Burg, and M. Mattauer (2000), Evolutionary model of the Himalaya-Tibet system: Geopem based on new modelling, geological and geophysical data, *Earth Planet. Sci. Lett.*, 174, 397–409, doi:10.1016/S0012-821X(99)00277-0.
- Crespo-Blanc, A. (1987), El macizo de Aracena (macizo Ibérico meridional): Propuesta de división sobre la base de nuevos datos estructurales y petrográficos, *Bol. Geol. Miner.*, 98, 507–515.
- Crespo-Blanc, A. (1992), Structure and kinematics of a sinistral transpressive suture between the Ossa-Morena and the South Portuguese zones, South Iberian Massif, *J. Geol. Soc.*, 149, 401–411, doi:10.1144/gsjgs.149.3.0401.
- Crespo-Blanc, A., and M. Orozco (1988), The southern Iberian Shear Zone: A major boundary in the Hercynian folded belt, *Tectonophysics*, 148, 221–227, doi:10.1016/0040-1951(88)90130-8.
- Dallmeyer, R. D., and C. Quesada (1992), Cadomian vs. Variscan evolution of the Ossa-Morena zone (SW Iberia): Field and  $^{40}\text{Ar}/^{39}\text{Ar}$  mineral age constraints, *Tectonophysics*, 216, 339–364, doi:10.1016/0040-1951(92)90405-U.
- Dallmeyer, R. D., P. E. Fonseca, C. Quesada, and A. Ribeiro (1993),  $^{40}\text{Ar}/^{39}\text{Ar}$  mineral age constraints to the tectonothermal evolution of the Variscan Suture in SW Iberia, *Tectonophysics*, 222, 177–194, doi:10.1016/0040-1951(93)90048-O.
- Dias, R., and A. Ribeiro (1995), The Ibero-Armorican Arc: A collision effect against an irregular continent?, *Tectonophysics*, 246, 113–128, doi:10.1016/0040-1951(94)00253-6.
- Díaz Azpiroz, M., C. Fernández, A. Castro, and M. El-Biad (2006), Tectono-metamorphic evolution of the Aracena metamorphic belt (SW Spain) resulting from ridge-trench interaction during Variscan plate convergence, *Tectonics*, 25, TC1001, doi:10.1029/2004TC001742.
- Dodson, M. H. (1973), Closure temperature in cooling geochronological and petrological systems, *Contrib. Mineral. Petrol.*, 40, 259–274, doi:10.1007/BF00373790.
- Dunlap, W. J., C. Teyssier, I. McDougall, and S. Baldwin (1991), Ages of deformation from K-Ar and  $^{39}\text{Ar}/^{40}\text{Ar}$  dating of white micas, *Geology*, 19, 1213–1216, doi:10.1130/0091-7613(1991)019<1213:AODFKA>2.3.CO;2.
- Ernst, W. G. (1979), Coexisting sodic and calcic amphiboles from high-pressure metamorphic belts and the stability field of barrositic amphiboles, *Mineral. Mag.*, 43, 269–278, doi:10.1180/minmag.1979.043.326.09.
- Evans, B. W. (1990), Phase relations of epidote-blueschists, *Lithos*, 25, 3–23, doi:10.1016/0024-4937(90)90003-J.
- Fonseca, P. E., and A. Ribeiro (1993), The tectonics of Beja-Acebuches Ophiolite; A major suture in the Iberian Variscan Fold Belt, *Geol. Rundsch.*, 82, 440–447, doi:10.1007/BF00212408.
- Fonseca, P. E., A. Araújo, N. Leal, and J. M. Munhá (1993), Variscan glaucophane-eclogites in the Ossa Morena Zone, *Terra Abstr. Suppl.*, 5(6/38), 11–12.
- Fonseca, P. E., J. M. Munhá, J. Pedro, F. M. Rosas, P. Moita, A. Araújo, and N. Leal (1999), Variscan ophiolites and high-pressure metamorphism in southern Iberia, *Ophioliti*, 24(2), 259–268.
- Gomes, M. C. (2000), Metamorfismo de Rochas Carbonatadas Silíceas da Região de Alvito (Alentejo, Sul de Portugal), Ph.D. thesis, 248 pp., Univ. of Coimbra, Coimbra, Portugal.
- Jesus, A. P., J. Munhá, A. Mateus, C. Tassinari, and A. P. Nutman (2007), The Beja layered gabbroic sequence (Ossa-Morena Zone, southern Portugal): Geochronology and geodynamic implications, *Geodin. Acta*, 20(3), 139–157, doi:10.3166/ga.20.139-157.
- Julivert, M., J. M. Fontbote, A. Ribeiro, and L. Conde (1974), Memória explicativa del Mapa Tectónico de la Península Ibérica y Baleares, scale 1:1000,000, 104 pp., Inst. Geol. y Minero de España, Madrid.
- Mac Gillavry, H. L. (1961), Deep or not Deep, fore-deep or “after-deep”?, *Geol. Mijnbouw*, 40, 133–148.
- Malavieille, J. (1993), Late orogenic extension in mountain belts: Insights from the Basin and Range and the Late Paleozoic Variscan belt, *Tectonics*, 12, 1115–1130, doi:10.1029/93TC01129.
- Marques, F. O., and P. R. Cobbold (1995), Development of highly non-cylindrical folds around rigid ellipsoidal inclusions in bulk simple shear regimes: Natural examples and experimental modelling, *J. Struct. Geol.*, 17, 589–602, doi:10.1016/0191-8141(94)00081-A.
- Marques, F. O., A. Mateus, and C. Tassinari (2002), The Late-Variscan fault network in central-northern Portugal (NW Iberia): A re-evaluation, *Tectonophysics*, 359, 255–270, doi:10.1016/S0040-1951(02)00514-0.
- Martínez, F. J., and I. G. Ibarguchi (1983), El metamorfismo en el Macizo Ibérico, in *Libro Jubilar J. M. Rios. Geología de España 1*, pp. 555–569, Publ. Inst. Geol. Mineiro España, Madrid, Spain.
- Matte, P. (1986), Tectonics and plate tectonic model for the Variscan belt of Europe, *Tectonophysics*, 126, 329–374, doi:10.1016/0040-1951(86)90237-4.
- Matte, P. (1991), Accretionary history and crustal evolution of the Variscan belt in Western Europe, *Tectonophysics*, 196, 309–337, doi:10.1016/0040-1951(91)90328-P.
- Matte, P., and A. Ribeiro (1975), Forme et orientation de l’ellipsoïde de déformation dans la virgation hercynienne de Galicie: Relation avec le plissement et hypothèses sur la genèse de l’arc Ibéro-Armoricain, *C. R. Acad. Sci.*, 280, 2825–2828.
- Ménard, G., and P. Molnar (1988), Collapse of a Hercynian Tibetan Plateau into a Late Paleozoic European Basin and Range province, *Nature*, 334, 235–237, doi:10.1038/334235a0.
- Monteiro Santos, F. A., J. Pous, E. Almeida, P. Queralt, A. Marcuello, H. Matias, and L. A. Mendes-Victor (1999), Electrical conductivity of the crust across the Ossa Morena and South Portuguese Zone suture—Preliminary results, *Tectonophysics*, 313, 449–462, doi:10.1016/S0040-1951(99)00209-7.
- Monteiro Santos, F. A., A. Mateus, A. Almeida, J. Pous, and L. A. Mendes-Victor (2002), Are some of the deep crustal conductive features found in SW Iberia caused by graphite?, *Earth Planet. Sci. Lett.*, 201, 353–367, doi:10.1016/S0012-821X(02)00721-5.
- Munhá, J. M., J. T. Oliveira, A. Ribeiro, V. Oliveira, C. Quesada, and R. Kerrich (1986), Beja-Acebuches Ophiolite characterization and geodynamic significance, *Maleo*, 2, 30.
- Norton, M. G. (1986), Late Caledonide extension in western Norway: A response to extreme crustal thickening, *Tectonics*, 5, 195–204, doi:10.1029/TC0051002p00195.
- Oliveira, J. T., M. Ramalho, and J. H. Monteiro (1992), Carta Geológica de Portugal à escala 1/500.000, Serv. Geol. de Portugal, Lisbon.
- Passchier, C. W., and R. A. J. Trouw (2005), *Microtectonics*, 366 pp., Springer, Berlin.
- Pereira, Z. (1999), Palinostigrafia do sector sudoeste da zona sul portuguesa, *Comun. Inst. Geol. Mineiro*, 86, 25–58.
- Pereira, Z., V. Oliveira, and J. T. Oliveira (2006), Palynostratigraphy of the Toca da Moura and Cabrela complexes, Ossa Morena Zone, Portugal: Geodynamic implications, *Rev. Palaeobot. Palynol.*, 139, 227–240, doi:10.1016/j.revpalbo.2005.07.008.
- Piçarra, J. M., and J. C. Gutiérrez-Marco (1992), Estudo dos graptólitos Silúricos do Flanco Oriental do Anticlinal de Moura-Ficalho (Sector de Montemor-Ficalho, Zona de Ossa Morena, Portugal), *Comun. Serv. Geol. Portugal*, 78, 23–29.
- Pin, C., J.-L. Paquette, and P. E. Fonseca (1999), 350 Ma (U-Pb Zircon) igneous emplacement age and Sr-Nd isotopic study of the Beja Gabbroic Complex (S. Portugal), *J. Conf. Abstr.*, 4(3), 1019.
- Pous, J., G. Muñoz, W. Heise, J. C. Melgarejo, and C. Quesada (2004), Electromagnetic imaging of Variscan crustal structures in SW Iberia: The role of interconnected graphite, *Earth Planet. Sci. Lett.*, 217, 435–450, doi:10.1016/S0012-821X(03)00612-5.
- Quesada, C. (1990), Ossa Morena Zone: An Introduction, in *Pre-Mesozoic of Geology of Iberia*, edited by D. Dallmeyer and E. Martínez-García, pp. 248–251, Springer, Berlin.
- Quesada, C. (1991), Geological constraints on the Paleozoic tectonic evolution of tectonostratigraphic Terranes in the Iberian Massif, *Tectonophysics*, 185, 225–245, doi:10.1016/0040-1951(91)90446-Y.
- Quesada, C. (1992), Evolución Tectónica del Macizo Ibérico (Una historia de crecimiento por acrecencia sucesiva de Terrenos durante el Proterozoico superior y el Paleozoico), in *Paleozoico Inferior de Ibero-América*, edited by J. G. Gutiérrez-Marco et al., pp. 173–190, Univ. de Extremadura, Badajoz, Spain.
- Quesada, C., F. Bellido, R. D. Dallmeyer, I. Gil Ibarguchi, J. T. Oliveira, A. Pérez-Estaun, A. Ribeiro, M. Rtbodyardet, and J. B. Silva (1991), Terranes within the Iberian Massif: Correlations with West African sequences, in *The West African Orogens and Circum-Atlantic Correlations*, edited by R. D. Dallmeyer and J. P. Lecorche, pp. 267–294, Springer, Berlin.
- Quesada, C., P. E. Fonseca, J. M. Munhá, J. T. Oliveira, and A. Ribeiro (1994), The Beja-Acebuches Ophiolite (southern Iberian Variscan Fold Belt): Geological characterization and geodynamic significance, *Bol. Geol. Mineiro*, 105, 3–49.
- Reddy, S. M., and G. J. Potts (1999), Constraining absolute deformation ages: The relationship between deformation mechanisms and isotope systematics, *J. Struct. Geol.*, 21, 1255–1265, doi:10.1016/S0191-8141(99)00332-2.
- Ribeiro, A., and E. Pereira (1986), Flake tectonics in the NW Iberia Variscides, *Maleo*, 2(13), 38.
- Ribeiro, A., M. T. Antunes, M. P. Ferreira, R. B. Rocha, A. F. Soares, G. Zbyszewski, F. Moitinho de Almeida, D. Carvalho, and J. H. Monteiro (1979), *Introdução à Geologia Geral do Portugal*, 114 pp., Serv. Geol. de Portugal, Lisbon.
- Ribeiro, A., C. Quesada, and R. D. Dallmeyer (1990), Geodynamic evolution of the Iberian Massif, in *Pre-Mesozoic of Geology of Iberia*, edited by D. Dallmeyer and E. Martínez-García, pp. 398–409, Springer, Berlin.
- Ribeiro, A., R. Dias, and J. B. Silva (1995), Genesis of the Ibero-Armorican Arc, *Geodin. Acta*, 8(4), 173–184.
- Ribeiro, A., et al. (2007), Geodynamic evolution of the SW Europe Variscides, *Tectonics*, 26, TC6009, doi:10.1029/2006TC002058.
- Ring, U., M. T. Brandon, S. D. Willett, and G. S. Lister (1999), Exhumation Processes, in *Exhumation Processes: Normal Faulting, Ductile Flow and Erosion*, edited by U. Ring et al., *Geol. Soc. Spec. Publ.*, 154, 1–27.
- Rosas, F. (2003), Estudo tectónico do sector de Viana do Alentejo-Alvito: evolução geodinâmica e modelação analógica de estruturas em afloramentos chave (ramo sul da Cadeia Varisca Ibérica - SW da Zona de Ossa-Morena), Ph.D. thesis, 354 pp., Univ. of Lisbon, Lisbon, Portugal.
- Rosas, F. M., F. O. Marques, S. Coelho, and P. E. Fonseca (2001), Sheath fold development in bulk simple shear: Analogous modeling of natural examples from the Southern Iberian Variscan Fold Belt, in *Tectonic Modeling: A Volume in Honor of Hans Ramberg*, edited by H. A. Koyi and N. S. Mancktelow, *Mem. Geol. Soc. Am.*, 193, 101–110.
- Rosas, F. M., F. O. Marques, A. Luz, and S. Coelho (2002), Sheath folds formed by drag induced by rotation of rigid inclusions in viscous simple shear flow: Nature and experiment, *J. Struct. Geol.*, 24, 45–55, doi:10.1016/S0191-8141(01)00046-3.
- Santos, J. F., J. Mata, F. Gonçalves, and J. M. Munhá (1987), Contribuição para o conhecimento geológico-petroológico da região de Santa Susana: O complexo vulcano-sedimentar da Toca da Moura, *Comun. Serv. Geol. Portugal*, 73, 29–48.

- Santos, J. F., A. Andrade, and J. M. Munhá (1990), Magmatismo Orogénico Varisco no Limite Meridional da Zona de Ossa-Morena, *Comun. Serv. Geol. Portugal*, 76, 91–124.
- Schermerhorn, L. J. G. (1971), An outline stratigraphy of the Iberian Pyrite Belt, *Bol. Geol. Min.*, 82, 239–268.
- Silva, J. B., and M. F. Pereira (2004), Transcurrent continental tectonics model for the Ossa-Morena Zone Neoproterozoic-Paleozoic evolution, SW Iberian massif, Portugal, *Int. J. Earth Sci.*, 93, 886–896, doi:10.1007/s00531-004-0424-5.
- Simancas, J. F., et al. (2003), the crustal structure of the transpressional Variscan Orogen of SW Iberia: The IBERSEIS deep seismic profile, *Tectonics*, 22(6), 1062, doi:10.1029/2002TC001479.
- Simancas, J. F., A. Tahiri, A. Azor, F. G. Lodeiro, D. J. M. Poyatos, and H. El Hadi (2005), The tectonic frame of the Variscan–Allegghanian orogen in southern Europe and northern Africa, *Tectonophysics*, 398, 181–198, doi:10.1016/j.tecto.2005.02.006.
- Steiger, R. H., and E. Jäger (1977), Subcommittee on geochronology: Convention on the use of decay constants in geo- and cosmochronology, *Earth Planet. Sci. Lett.*, 36, 359–362, doi:10.1016/0012-821X(77)90060-7.
- Teixeira, C. (1981), *Geologia de Portugal—Precâmbri-co e Paleozóico*, 229 pp., Fundação Calouste Gulbenkian, Lisbon.
- 
- M. Ballèvre, Géosciences-Rennes, UMR6118, Université de Rennes, Campus de Beaulieu, CNRS, F-35042 Rennes, France.
- F. O. Marques, CGUL-IDL, Faculdade Ciências, Universidade Lisboa, P-1749-016 Lisbon, Portugal.
- F. M. Rosas, Departamento de Geologia, Faculdade Ciências, Universidade Lisboa, Campo Grande, Edifício C6, Piso 4, Lisbon P-1749-016, Portugal. (frosas@fc.ul.pt)
- C. Tassinari, Centro de Pesquisas Geocronológicas da Universidade de São Paulo, São Paulo, Brazil, CEP 05508-080.